

FINAL REPORT

Electrochemical Demilitarization Of Energetics

SERDP Project WP-2614

MAY 2018

Dr. Mark E. Fuller
Aptim Federal Services

Distribution Statement A

This document has been cleared for public release



Page Intentionally Left Blank

This report was prepared under contract to the Department of Defense Strategic Environmental Research and Development Program (SERDP). The publication of this report does not indicate endorsement by the Department of Defense, nor should the contents be construed as reflecting the official policy or position of the Department of Defense. Reference herein to any specific commercial product, process, or service by trade name, trademark, manufacturer, or otherwise, does not necessarily constitute or imply its endorsement, recommendation, or favoring by the Department of Defense.

Page Intentionally Left Blank

REPORT DOCUMENTATION PAGE				Form Approved OMB No. 0704-0188	
<p>The public reporting burden for this collection of information is estimated to average 1 hour per response, including the time for reviewing instructions, searching existing data sources, gathering and maintaining the data needed, and completing and reviewing the collection of information. Send comments regarding this burden estimate or any other aspect of this collection of information, including suggestions for reducing the burden, to the Department of Defense, Executive Services and Communications Directorate (0704-0188). Respondents should be aware that notwithstanding any other provision of law, no person shall be subject to any penalty for failing to comply with a collection of information if it does not display a currently valid OMB control number.</p> <p>PLEASE DO NOT RETURN YOUR FORM TO THE ABOVE ORGANIZATION.</p>					
1. REPORT DATE (DD-MM-YYYY) 03-27-2018		2. REPORT TYPE SERDP Final Report		3. DATES COVERED (From - To) July 2016 - April 2018	
4. TITLE AND SUBTITLE Electrochemical Demilitarization Of Energetics			5a. CONTRACT NUMBER W912HQ-16-P-0008		
			5b. GRANT NUMBER NA		
			5c. PROGRAM ELEMENT NUMBER NA		
6. AUTHOR(S) Fuller, Mark E., Ph.D.			5d. PROJECT NUMBER WPSEED-2614		
			5e. TASK NUMBER NA		
			5f. WORK UNIT NUMBER NA		
7. PERFORMING ORGANIZATION NAME(S) AND ADDRESS(ES) Aptim Federal Services (formerly CB&I Federal Services) 17 Princess Road Lawrenceville, NJ 08648			8. PERFORMING ORGANIZATION REPORT NUMBER WP-2614		
9. SPONSORING/MONITORING AGENCY NAME(S) AND ADDRESS(ES) Strategic Environmental Research and Development Program 4800 Mark Center Drive, Suite 17D08 Alexandria, VA 22350-3600			10. SPONSOR/MONITOR'S ACRONYM(S) SERDP		
			11. SPONSOR/MONITOR'S REPORT NUMBER(S) WP-2614		
12. DISTRIBUTION/AVAILABILITY STATEMENT Distribution Statement A: Approved for Public Release, Distribution is Unlimited					
13. SUPPLEMENTARY NOTES None					
14. ABSTRACT The key objective of this project was to demonstrate electrochemical treatment of several representative explosive and propellant compounds at the bench-scale. Specific attention was given to determining the overall rates of treatment, delineating the major transformation products of the process, performing carbon and nitrogen mass balances, and assessing the ability to effectively treat slurried and solid phase explosives and propellants. The technical approach included screening level testing to select the appropriate electrode / electrolyte combination and operational parameters to effectively destroy the target energetic materials (e.g., RDX from Composition B and nitrocellulose). This was followed by larger bench-scale testing over a longer duration to evaluate treatment effectiveness, generate reaction rates, and determine any electrode fouling or failure possibilities. The proposed technology potential offers DoD a means to address demilitarization wastestreams in a manner that does not require the use of dangerous reactive chemicals or environmentally unfriendly processes.					
15. SUBJECT TERMS RDX, explosive, munition, nitrocellulose, propellant, electrochemical, demilitarization, degradation					
16. SECURITY CLASSIFICATION OF:			17. LIMITATION OF ABSTRACT UU	18. NUMBER OF PAGES 69	19a. NAME OF RESPONSIBLE PERSON Dr. Mark E. Fuller
a. REPORT U	b. ABSTRACT U	c. THIS PAGE U			19b. TELEPHONE NUMBER (Include area code) 609-895-5348

Reset

Standard Form 298 (Rev. 8/98)
Prescribed by ANSI Std. Z39.18

Page Intentionally Left Blank

TABLE OF CONTENTS

LIST OF TABLES	III
LIST OF FIGURES	IV
ACRONYM LIST	VI
ACKNOWLEDGEMENTS	VIII
EXECUTIVE SUMMARY	9
1.0 PROJECT OBJECTIVES AND INTRODUCTION.....	11
1.1 PROJECT OBJECTIVES	11
1.2 INTRODUCTION AND BACKGROUND	12
1.2.1 Demilitarization waste streams.....	12
1.2.2 Description of electrochemical processes.	12
2.0 PROJECT TASKS.....	15
2.1 TASK 1 – ANODE SELECTION AND SYSTEM ASSEMBLY	15
2.1.1 Goal and Introduction.....	15
2.1.2 Methods, Results, and Discussion.....	15
2.2 TASK 2 – DEGRADATION OF RDX IN UNDIVIDED CELL CONFIGURATION.....	17
2.2.1 Goal and Introduction.....	17
2.2.2 Comparison of RDX degradation with different anodes.....	18
2.2.3 Degradation of nitrate and nitrite.....	24
2.2.4 Effect of electrolyte concentration and flow rate on RDX degradation.	28
2.3 TASK 3 – DEGRADATION OF RDX IN DIVIDED CELL CONFIGURATION	30
2.3.1 Goal and Introduction.....	30
2.3.2 RDX degradation at constant current.....	31
2.4 TASK 4 – DEGRADATION OF NITROCELLULOSE IN DIVIDED CELL CONFIGURATION	35
2.4.1 Goal and Introduction.....	35
2.4.2 System retrofit.	35
2.4.3 Nitrocellulose analysis.....	35
2.4.4 Bulk hydrolysis of NC fines.....	38
2.4.5 Determination of minimum voltage to generate steady current	39
2.4.6 Cathodic production of hydroxide	42
2.4.7 Cathodic degradation of nitrite and nitrate.....	42
2.4.8 Cathodic degradation of NC fines	44
2.5 TASK 5 – LONGER-TERM DEGRADATION OF RDX IN DIVIDED CELL CONFIGURATION.....	54
2.5.1 Goal and Introduction.....	54
2.5.2 RDX degradation at constant voltage.....	54
2.5.3 Multirun testing of RDX degradation	56
3.0 CONCLUSIONS AND IMPLICATIONS FOR FUTURE RESEARCH	59
3.1 KEY RESULTS	59
3.2 SUGGESTED FOLLOW-ON WORK	60
4.0 REFERENCES CITED	61
5.0 APPENDICES	64

LIST OF TABLES

Table 2.1-1.	Electrochemical test system parts list.	16
Table 2.2-1.	Best fit RDX degradation rate coefficients (k ; 1/h) and current efficiencies for the four anodes tested.	22
Table 2.2-2.	Effects of electrolyte concentration and flow rate on RDX degradation with the BDD and IrO ₂ anodes in the undivided cell configuration.	29
Table 2.3-1.	Anodic and cathodic RDX degradation with the BDD and IrO ₂ systems in the divided cell configuration.	33
Table 2.4-1.	Comparison of cost of bulk NC hydrolysis and electrochemical NC degradation based on alkali requirement.	53
Table 2.5-1.	RDX degradation rate confidents and other parameters for experiments with the IrO ₂ anode and SS cathode at a constant voltage or constant current.	56

LIST OF FIGURES

Figure 1-1.	Project flowchart.....	11
Figure 2.1-1.	Photograph of the electrochemical test system.....	16
Figure 2.2-1.	Illustration of the undivided cell configuration.	17
Figure 2.2-2.	Average test solution pH over time for the various anodes operated in the undivided cell configuration (n = 2 for each anode).....	20
Figure 2.2-3.	Degradation of RDX during experiments using the four different anodes (n=2 for each anode). 21	
Figure 2.2-4.	HPLC chromatogram at 0 hr (top) and 8 hr (bottom) for one of the RDX degradation experiments using the BDD anode showing appearance of unknown peaks (red circles).....	21
Figure 2.2-5.	Changes in RDX, nitrite, and nitrate expressed in mM nitrogen during experiments using the four different anodes (n = 2 for each anode).	23
Figure 2.2-6.	Changes in the pH of the test solution during degradation of nitrate using the BDD and RuO ₂ anodes.	25
Figure 2.2-7.	Degradation of nitrate and production of nitrite during experiments using the BDD and RuO ₂ anodes.	26
Figure 2.2-8.	Degradation of nitrite and production of nitrate during experiments using the BDD and RuO ₂ anodes.	27
Figure 2.3-1.	Illustration of the divided cell configuration.	30
Figure 2.3-2.	Effect of pH neutralization at time of sample collection on the calculated cathodic RDX degradation rate coefficient (top) and NDAB formation (bottom) in the BDD system.	34
Figure 2.4-1.	Illustration of the retrofitted electrochemical test system.....	36
Figure 2.4-2.	Photographs of the retrofitted electrochemical system (top) and the in-line strainer (bottom). ...	37
Figure 2.4-3.	Production of nitrite and nitrate (top) and calculated NC degradation rates (bottom) during batch alkaline hydrolysis of NC with three different initial hydroxide concentrations.....	39
Figure 2.4-4.	Plots of voltage vs. current in the BDD electrode system (top) and the IrO ₂ electrode system (bottom).....	41
Figure 2.4-5.	Cathodic degradation of nitrite (top) and nitrate (bottom) in the IrO ₂ electrode system.....	43
Figure 2.4-6.	Denitration of NC during the first test based on measured mass of nitrogen released (nitrite plus nitrate) (top) and corrected mass of nitrogen released (bottom) the IrO ₂ electrode system.	48
Figure 2.4-7.	Denitration of NC during the second test based on measured nitrite plus nitrate released (top) and corrected mass of nitrogen released (bottom) the IrO ₂ electrode system.	49
Figure 2.4-8.	Production of nitrite and nitrate during alkaline hydrolysis of NC in a flow through configuration with an initial hydroxide concentration of 0.3 N.	50
Figure 2.4-9.	Changes in hydroxide concentration over time during alkaline hydrolysis of NC in a flow through configuration with an initial hydroxide concentration of 0.3 N.....	50
Figure 2.4-10.	Comparison of nitrate and nitrite production during alkaline hydrolysis of NC with 0.3 N hydroxide (added as NaOH) and electrochemically generated hydroxide in a flow through configuration.	51
Figure 2.4-11.	Comparison of hydroxide molarity during alkaline hydrolysis with 0.3 N hydroxide (added as NaOH) and electrochemically generated hydroxide in a flow through configuration.....	51

Figure 2.4-12. Comparison of the NC denitration rate (expressed as percent of the initial nitrogen in the NC released) during alkaline hydrolysis with 0.3 N hydroxide (added as NaOH) and electrochemically generated hydroxide in a flow through configuration.....	52
Figure 2.5-1. Cathodic transformation of RDX in the divided cell configuration with the IrO ₂ anode and SS cathode at a constant voltage of 4 V.	55
Figure 2.5-2. Degradation of NDAB, nitrite, and nitrate in the divided cell configuration with the IrO ₂ anode and SS cathode at a constant voltage of 4 V.	56
Figure 2.5-3. RDX degradation rate coefficient for each test during the longer term evaluation.	58
Figure 2.5-4. Concentration of nitrite and NDAB, and the nitrogen mass balance, at the end of each test during the longer term evaluation.	58

ACRONYM LIST

A	amp
BDD	boron doped diamond
°C	degree Celsius
cm	centimeter
COD	chemical oxygen demand
d	day
DNAN	2,4-dinitroanisole
DPD	diethyl-p-phenylenediamine
DNX	1,3,5-hexahydro-1,3-dinitroso-5-nitro-triazine
DoD	Department of Defense
DSA	dimensionally stable anodes
g	gram
g	gravity
h	hour
HMX	1,3,5,7-tetranitro-1,3,5,7-tetrazocane
IHE	insensitive high explosives
IrO ₂	iridium dioxide
L	liter
μ	micro
m	milli or meter
M	molar
MC	munitions constituents
min	minute
mL	milliliter
mm	millimeter
MMO	mixed-metal oxide
MNX	1,3,5-hexahydro-1-nitroso-3,5-dinitro-1,3,5-triazine
mol	mole
n	nano
NC	nitrocellulose
NDAB	4-nitro-2,4-diazabutanal
NQ	nitroguanidine
NTO	3-nitro-1,2,4-triazol-5-one
OB/OD	open burn/open detonation
RDX	1,3,5-hexahydro-1,3,5-trinitro-1,3,5-triazine
rpm	revolutions per minute
RuO ₂	ruthenium dioxide
SE	standard error
SERDP	Strategic Environmental Research and Development Program
SnO ₂	tin oxide
SS	stainless steel
TNT	2,4,6-trinitrotoluene
TNX	1,3,5-hexahydro-1,3,5-trinitroso-1,3,5-triazine
TOC / TC	total organic carbon / total carbon
UV	ultraviolet
wt	weight

REPORT DOCUMENTATION PAGE				Form Approved OMB No. 0704-0188	
<p>The public reporting burden for this collection of information is estimated to average 1 hour per response, including the time for reviewing instructions, searching existing data sources, gathering and maintaining the data needed, and completing and reviewing the collection of information. Send comments regarding this burden estimate or any other aspect of this collection of information, including suggestions for reducing the burden, to the Department of Defense, Executive Services and Communications Directorate (0704-0188). Respondents should be aware that notwithstanding any other provision of law, no person shall be subject to any penalty for failing to comply with a collection of information if it does not display a currently valid OMB control number.</p> <p>PLEASE DO NOT RETURN YOUR FORM TO THE ABOVE ORGANIZATION.</p>					
1. REPORT DATE (DD-MM-YYYY) 03-27-2018		2. REPORT TYPE Final		3. DATES COVERED (From - To) July 2016 - April 2018	
4. TITLE AND SUBTITLE Electrochemical Demilitarization Of Energetics			5a. CONTRACT NUMBER W912HQ-16-P-0008		
			5b. GRANT NUMBER NA		
			5c. PROGRAM ELEMENT NUMBER NA		
6. AUTHOR(S) Fuller, Mark E., Ph.D.			5d. PROJECT NUMBER WPSEED-2614		
			5e. TASK NUMBER NA		
			5f. WORK UNIT NUMBER NA		
7. PERFORMING ORGANIZATION NAME(S) AND ADDRESS(ES) Aptim Federal Services (formerly CB&I Federal Services) 17 Princess Road Lawrenceville, NJ 08648			8. PERFORMING ORGANIZATION REPORT NUMBER NA		
9. SPONSORING/MONITORING AGENCY NAME(S) AND ADDRESS(ES) Strategic Environmental Research and Development Program 4800 Mark Center Drive, Suite 17D08 Alexandria, VA 22350-3600			10. SPONSOR/MONITOR'S ACRONYM(S) SERDP		
			11. SPONSOR/MONITOR'S REPORT NUMBER(S) NA		
12. DISTRIBUTION/AVAILABILITY STATEMENT Distribution Statement A: Approved for Public Release, Distribution is Unlimited					
13. SUPPLEMENTARY NOTES None					
14. ABSTRACT The key objective of this project was to demonstrate electrochemical treatment of several representative explosive and propellant compounds at the bench-scale. Specific attention was given to determining the overall rates of treatment, delineating the major transformation products of the process, performing carbon and nitrogen mass balances, and assessing the ability to effectively treat slurried and solid phase explosives and propellants. The technical approach included screening level testing to select the appropriate electrode / electrolyte combination and operational parameters to effectively destroy the target energetic materials (e.g., RDX from Composition B and nitrocellulose). This was followed by larger bench-scale testing over a longer duration to evaluate treatment effectiveness, generate reaction rates, and determine any electrode fouling or failure possibilities. The proposed technology potential offers DoD a means to address demilitarization wastestreams in a manner that does not require the use of dangerous reactive chemicals or environmentally unfriendly processes.					
15. SUBJECT TERMS RDX, explosive, munition, nitrocellulose, propellant, electrochemical, demilitarization, degradation					
16. SECURITY CLASSIFICATION OF:			17. LIMITATION OF ABSTRACT UU	18. NUMBER OF PAGES 61	19a. NAME OF RESPONSIBLE PERSON Dr. Mark E. Fuller
a. REPORT U	b. ABSTRACT U	c. THIS PAGE U			19b. TELEPHONE NUMBER (Include area code) 609-895-5348

Reset

Standard Form 298 (Rev. 8/98)
Prescribed by ANSI Std. Z39.18

ACKNOWLEDGEMENTS

This SERDP Project was a collaborative effort among Dr. Mark E. Fuller (Aptim) and Dr. Charles E. Schaefer (CDMSmith). We would also like to thank Dr. Paul Koster van Groos for his assistance with data analysis, and Ms. Christina Andaya (Aptim) for all her efforts with the laboratory experiments during this project.

We gratefully acknowledge SERDP for their financial support, and Dr. Robin Nissan, the Weapon Platforms Program Manager at SERDP, for his guidance and support during this project.

EXECUTIVE SUMMARY

Objective: This SERDP SEED project was a collaborative effort among scientists at Aptim Federal Services (formerly CB&I Federal Services) and CDM Smith. The key technical objective of this project was to demonstrate electrochemical treatment of several representative explosive and propellant compounds at the bench-scale. Specific attention was given to determining the overall rates of treatment, delineating the major breakdown products of the process, performing carbon and nitrogen mass balances, and assessing the ability to effectively treat solid phase propellants.

Technical Approach: This project used RDX as a representative explosive compound and nitrocellulose as a representative solid phase propellant. Several types of mixed metal oxide (MMO) anodes, and well as a boron doped diamond (BDD) anode were screen. Both undivided and divided electrochemical cell configurations were tested, and constant current and constant voltage conditions were evaluated. Chemical analyses were performed to monitor both the degradation of the parent compound, and the formation/destruction of possible breakdown products. A longer term experiment was also conducted to assess electrode longevity and changes in efficiency.

Key Results: This project produced solid proof-of-concept data that supports further investigation of electrochemical demilitarization of explosives and energetics. This project used a small-scale electrochemical system and single representative compounds (RDX and NC) to minimize the analytical complexity and allow multiple variables to be clearly compared.

For dissolved RDX (as a representative explosive), the key results of this project were as follows:

- In an undivided cell configuration with constant current:
 - Electrochemical degradation of dissolved RDX was demonstrated with both BDD and MMO anodes coupled to stainless steel (SS) cathodes.
 - Degradation rates were slightly higher with the BDD anode than with the MMO anodes, but more net RDX breakdown products (nitrite and nitrate) were produced with the BDD anode.
 - Modest changes in electrolyte concentration (10-fold) and flow rate (2-fold) only resulted in 10 to 20% changes in the RDX degradation rate coefficient.

- In a divided cell configuration with constant current:
 - Both anodic and cathodic degradation of dissolved RDX was demonstrated with BDD anode coupled to a SS cathode. This indicates the potential for sequential cathodic/anodic treatment with increased degradation efficiency (e.g., higher mass degraded per unit of energy expended).
 - Robust RDX degradation was only observed cathodically with an IrO₂ anode coupled to a SS cathode.

- Cathodic degradation rates were higher in the divided configuration compared to the undivided configuration, which was attributed to the more alkaline conditions in the catholyte in the divided cell configuration.
- In a divided cell configuration with constant voltage:
 - Cathodic RDX degradation rates with an IrO₂ anode coupled to a SS cathode were relatively stable over repeated tests, indicating good longevity of the electrodes.

For NC, this project performed the first known demonstration of alkaline hydrolysis of solid nitrocellulose via electrochemically generated hydroxide using an IrO₂ anode coupled to a SS cathode operated in divided cell configuration with constant voltage. The nitrite, nitrate, and carbonaceous breakdown products generated were partially degraded as the NC was hydrolyzed. The preliminary data indicated that the electrochemical process was 50-60% more efficient than bulk alkaline hydrolysis based on the rate of NC denitration, which would be expected to result in lower cost per kg of NC treated.

Benefits: This research has added to the scientific knowledge base regarding potential technologies for demilitarization activities. While further testing is needed to optimize the conditions and generate information for cost-benefit analysis, these preliminary findings provide proof-of-concept that electrochemical processes can be employed to degrade explosives and propellants to non-toxic products. This approach would also provide an added level of worker safety, as bulk chemicals (e.g., caustic) do not need to be stored or handled.

1.0 PROJECT OBJECTIVES AND INTRODUCTION

1.1 Project Objectives

The key technical objective of this project was to demonstrate electrochemical treatment of several representative explosive and propellant compounds at the bench-scale. The overall goal was to evaluate which electrochemical designs would be effective for explosive and propellant treatment with respect to specific anodes and cell configurations.

Specific attention was given to determining the overall rates of treatment, delineating the major breakdown products of the process (directed towards understanding the mechanism of degradation), performing mass balances, and assessing the ability to effectively treat solid phase propellants.

Figure 1-1 presents the general experiment plan this project followed. Task details and results are presented in the following sections of the report.

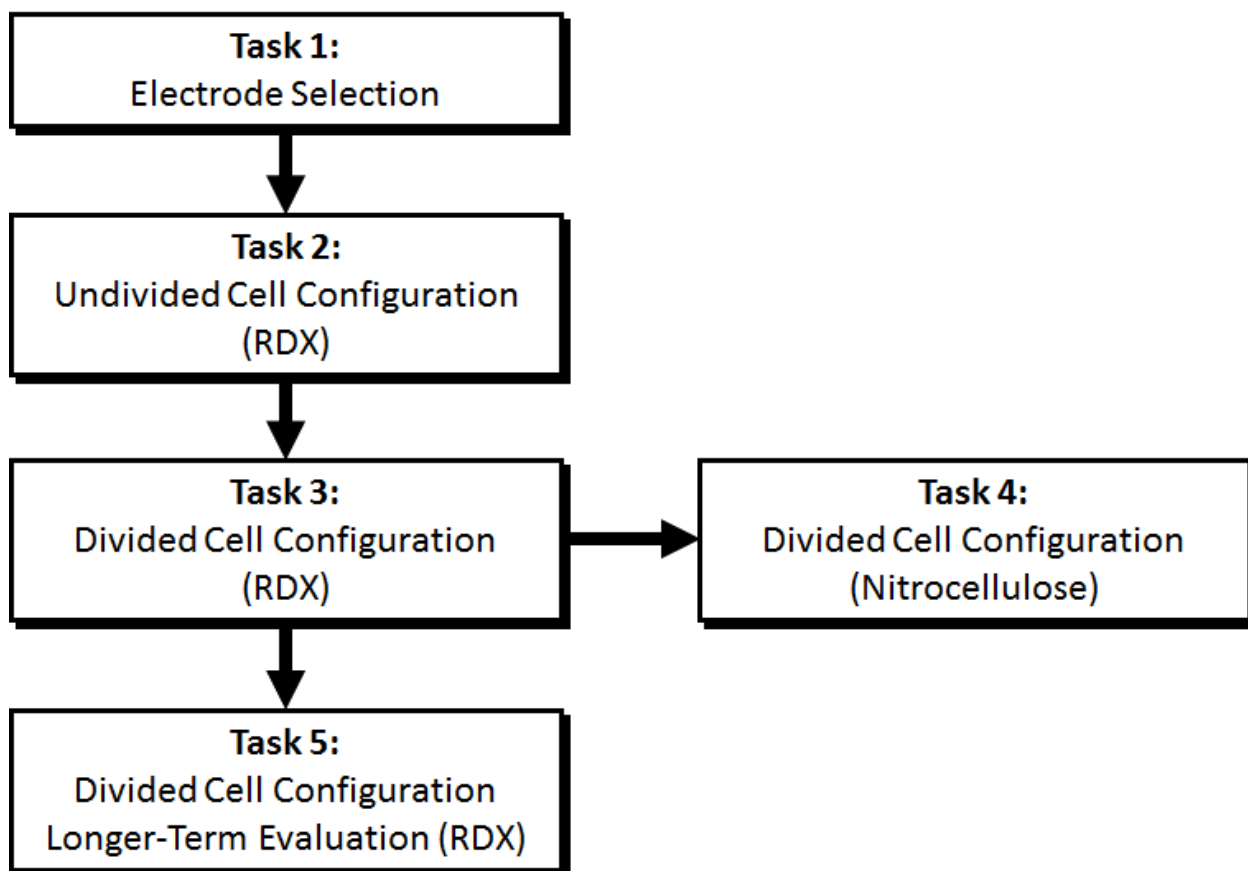


Figure 1-1. Project flowchart.

1.2 Introduction and Background

1.2.1 Demilitarization waste streams.

DoD has an ongoing need to safely dispose of a variety of munitions that are no longer usable (e.g., obsolete, unstable). Several DoD entities also serve as the “go to” resource for disposal of confiscated contraband fireworks and pyrotechnics (Dr. Randall Cramer, personal communication). The standard practice for demilitarization of these munitions has been through open burn / open detonation (OB/OD), but this option has become less attractive due to negative reactions of local communities, as well as concerns about safety and/or potential environmental contamination with residuals. Some approaches involve alternative munition destruction methods (e.g., contained detonation, contained burn) (35). Other demilitarization practices involve removal of the energetic material from a munition via physical or liquid extraction (e.g., water jet cutting, cryofracturing, meltout), followed by cleaning and recycling of the metal components and reuse/recycling or additional treatment of the explosives and propellant wastestream using thermal, chemical, or biological methods (29, 35). This SEED project was focused on demonstrating proof-of-concept of an electrochemical processes to degrade the explosives or propellants in a safe and environmentally friendly manner.

1.2.2 Description of electrochemical processes.

Electrochemical cells (ECs) have been used to treat a wide range of organic and inorganic contaminants. The high level of treatment and relative low energy input highlight the promising nature of an electrochemical approach. The treatment mechanisms for contaminants in water include direct and indirect oxidation/reduction as well as electrocoagulation and precipitation of suspended solids. Electrolysis of water can produce several reactive oxygen species (ROS) by oxidation of water at the anode, such as hydroxyl radicals ($\bullet\text{OH}$), ozone (O_3), superoxide radicals ($\bullet\text{O}_2^-$), and hydrogen peroxide (H_2O_2). Chlorine-based oxidants (e.g., hypochlorite) also can form if chloride is present in the water. In addition, if the electrochemical cell operated in a divided configuration, both low and high pH conditions can be generated in the anodic and cathodic loops, respectively, thus promoting acid and alkaline hydrolysis reactions. These processes occur simultaneously within the EC cell, which result in the disinfection of water, destruction of contaminants, and reduction of BOD/COD and suspended solids (15, 20, 21).

One key for efficient electrolytic oxidation is choice of anode material. Dimensionally Stable Anodes (DSA), which include the sub-category of mixed metal oxide (MMO) anodes, have high corrosion resistance and physical/chemical stability, under high positive potentials. These electrodes are thermally prepared with a titanium substrate covered by metallic oxides. Coatings on titanium include TiO_2 , IrO_2 , RuO_2 and Ta_2O_5 . Combinations such as $x(\text{TiO}_2)/y(\text{RuO}_2)$ and $x(\text{IrO}_2)/y(\text{Ta}_2\text{O}_5)$ are currently marketed and used as electrodes for the chlor-alkali industry (27). Ruthenium oxide (RuO_2) is widely used for Cl_2 and O_2 production. RuO_2 has good conductivity, good barrier properties against oxygen diffusion, and good stability at room temperature as high as 800°C . Ruthenium and ruthenium oxide have also excellent chemical stability (38).

It is possible to produce hydroxyl radicals ($\text{OH}\bullet$), which are strong oxidizing agents, by using MMO anodes. Water oxidation at MMO anodes produces adsorbed hydroxyl radicals, which can potentially evolve towards the formation of chemisorbed oxygen and/or oxygen evolution. Direct

evidence for the occurrence of oxygen evolution by means of adsorbed oxygen has been proved with ruthenium and iridium oxide electrodes using labeled oxygen and mass spectrometry measurements (31). Oxidizable organics can be oxidized by adsorbed hydroxyl radicals and/or by adsorbed oxygen. Ongoing projects at Aptim and CDM Smith are evaluating the use of MMO anodes for both treatment of perfluorinated compounds in groundwater, and for disinfecting surface water for drinking at NAS Lemoore (**Figure 1-2**).

Figure 1-2. Pilot-scale electrochemical system APTIM evaluated for drinking water disinfection at Naval Air Station (NAS) Lemoore.



Boron-doped diamond (BDD) electrodes have shown great promise for treating many types of wastewaters. The boron doping allows the diamond to become a semiconductor, while retaining a high level of chemical inertness (5). BDD electrodes also are resistant to corrosion, with expected lifetimes in excess of five years (17). BDD electrodes have the widest known electrochemical window prior to water dissociation. This large potential window (~3.5 V) facilitates the anodic generation of several strong oxidizing agents (e.g., hydroxyl radicals, hydrogen peroxide, persulfate) with a high current efficiency (8, 11). However, one challenge with BDD anodes is that these anodes promote the oxidation of chloride to perchlorate (2, 30). They are also subject to possible persulfate modification/degradation in the presence of high sulfate concentrations under acidic conditions.

The generation of oxidants by both MMO and BDD anodes can greatly enhance the observed degradation rates of target contaminants, as generation of these oxidants can facilitate reactions in the bulk aqueous phase, thereby eliminating the kinetically limiting step (in many cases) of contaminant sorption to the anode. For treatment of non-aqueous or slurried compounds typical

of demilitarization processes, the anodically generated oxidants likely will provide a substantial treatment benefit. The generated oxidants are expected to enhance dissolution of non-aqueous components, and facilitate an overall increase in the observed treatment rate.

In addition to anode material, another key factor when considering electrochemical treatment is cell configuration – namely undivided versus divided electrochemical cells. Several recent studies suggest that divided electrochemical cell configurations, which may include sequential anodic-cathodic treatment, can enhance removal of COD and organic contaminants (12, 24, 30, 34, 39). In the context of treating energetic compounds such as RDX, divided cell configuration can 1) limit the scavenging of reactive oxidative species formed at the anode, 2) facilitate the direct reductive transformation at the cathode (4, 7), and 3) facilitate alkaline hydrolysis in the high pH catholyte (32).

2.0 PROJECT TASKS

2.1 Task 1 – Anode Selection and System Assembly

2.1.1 Goal and Introduction

In light of the overall project goal

To evaluate which electrochemical designs would be effective for explosive and propellant treatment with respect to specific anodes and cell configurations.

the focus of this task was to select a variety of MMO anodes to test along with the BDD anode, and to design and assemble the bench-scale system for running degradation experiments.

2.1.2 Methods, Results, and Discussion

2.1.2.1 Anode selection.

The anodes used during this project were selected based on a thorough literature review of past research, combined with past experience with electrochemical processes for the degradation of other contaminants and for water disinfection (see section 1.2.2 above). The anodes used are listed in **Table 2.1-1**, and include three MMO anodes and a BDD anode. For simplicity, the MMO anodes Ti/IrO₂, Ti/RuO₂ and Ti/SnO₂ are referred to hereafter based only on the transition metal they contain, hence IrO₂, RuO₂, and SnO₂, respectively. Each anode was paired with a stainless steel (SS) cathode during all testing. The wetted surface area of each electrode use was 10 cm².

2.1.2.2 Test system design and assembly.

This project utilized a microcell electrochemical cell, which allowed experiments to be performed with relatively small working volumes (0.2 – 0.4 L). A photograph of the base system is shown in **Figure 2.1-1**, and a parts list is presented in **Table 2.1-1**. The base system consisted of the electrochemical cell placed inside a protective case, a power supply, a peristaltic pump to circulate the test solution, a flow meter to monitor flow rates, and reservoirs for the test solution(s). Standard Tygon tubing was used for the initial testing, with norprene tubing used in the pump heads. Minimal loss of RDX was observed with both tubing types. All other fittings were polypropylene. Test solutions were placed in HDPE plastic bottles unless otherwise noted. Glass beakers larger than the plastic bottles were used as secondary containment.

Item	Vendor	Part Number
Micro Flow Cell Base Unit ¹	ElectroCell North America, Inc.	MFCB
Nafion 117 membrane	ElectroCell North America, Inc.	4-40102-00
Electrodes		
Stainless steel (type 316)	ElectroCell North America, Inc.	4-40004-01
Boron-doped diamond	ElectroCell North America, Inc.	4-40001-03
Iridium oxide on titanium, Grade 1	Electrochem Technologies & Materials, Inc.	EMMO-IRO-TI1-MS-MIC
Ruthenium oxide on titanium, Grade 1	Electrochem Technologies & Materials, Inc.	EMMO-RUO-TI1-HS-MIC
Iridium coated MMO anode with SnO ₂ topcoat	Electrochem Technologies & Materials, Inc.	EMMO-SNO-IRO-TI1-MS-MIC
E3633A 200W Power supply	Agilent	E3633A
Valved Acrylic Variable-Area Flowmeter	Cole-Parmer	UJ-32461-34
Masterflex, L/S Variable-Speed Drive w/Remote I/O, 100rpm	Cole-Parmer	EW-07528-30
Masterflex, Easy-Load II Head for High-Performance Tubing	Cole-Parmer	EW-077200-62
Masterflex, noreprene tubing L/S 24	Cole-Parmer	06404-24
Chemical resistant, clear Tygon tubing	McMaster-Carr	5103K34

¹Micro Flow Cell Base Unit contains the following:

- 2 - Stainless steel endplates
- 2 - PTFE flow frames
- 2 - PTFE end frames
- 2 - Viton electrode gaskets
- 2 - Viton end frame gaskets
- 2 - Viton membrane gaskets
- 1 - Set of PTFE guide pins and SS hardware

Table 2.1-1. Electrochemical test system parts list.

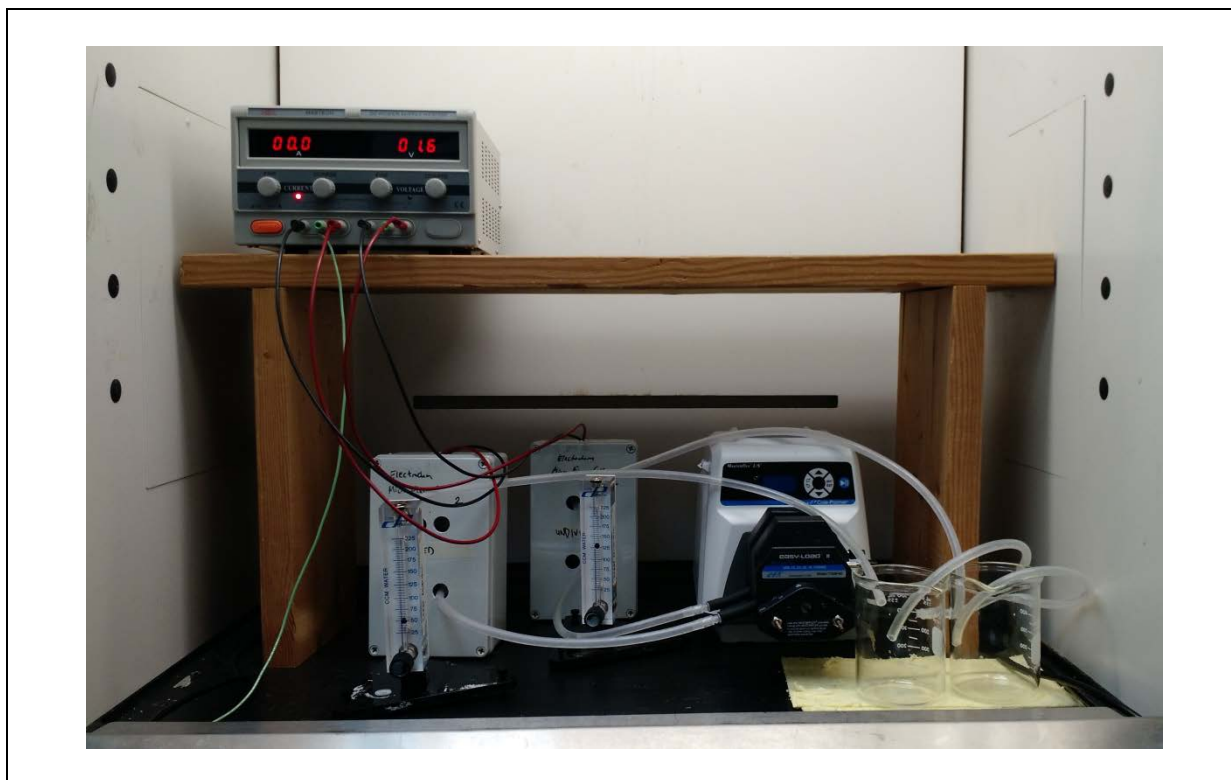


Figure 2.1-1. Photograph of the electrochemical test system.

2.2 Task 2 – Degradation of RDX in undivided cell configuration

2.2.1 Goal and Introduction

In light of the overall project goal

To evaluate which electrochemical designs would be effective for explosive and propellant treatment with respect to specific anodes and cell configurations.

The focus of this task was to evaluate the degradation of RDX using the MMO and BDD anodes with the electrochemical cell in the undivided configuration. In this configuration, a single test solution passes through the microcell and is exposed to the anode and the cathode simultaneously, as illustrated in **Figure 2.2-1**. Various parameters were varied during this task to evaluate their effects on RDX degradation kinetics.

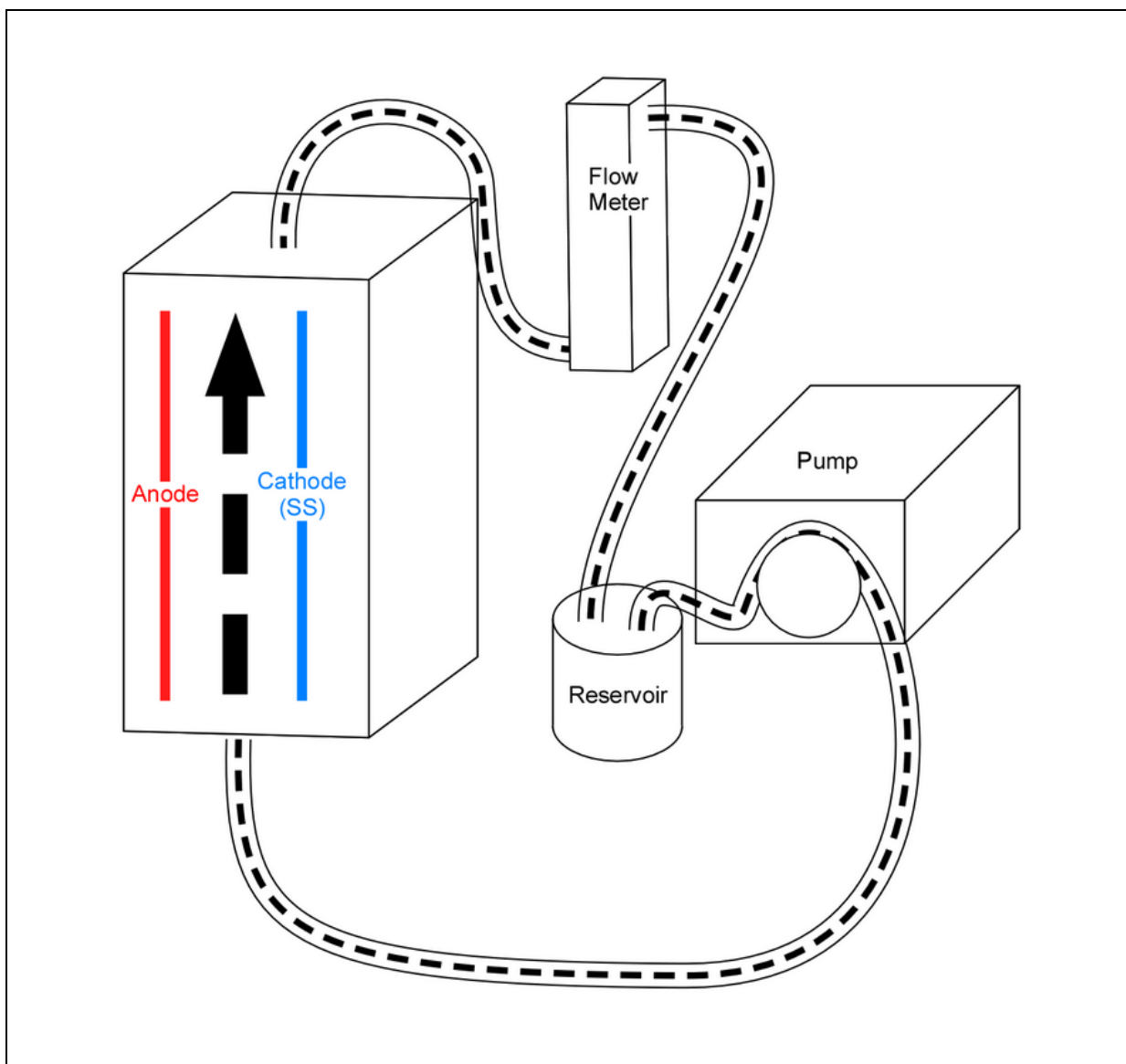


Figure 2.2-1. Illustration of the undivided cell configuration.

2.2.2 Comparison of RDX degradation with different anodes.

2.2.2.1 Methods.

All three MMO anodes and the BDD boron-doped diamond anode (BDD) were included in the initial testing. Testing was done with the following basic parameters:

-Configuration:	Undivided flow cell
-RDX:	Approximately 30 to 40 mg/L
-Cathode:	SS
-Gap:	4 mm (distance between anode and cathode)
-Electrode Area:	10 cm ²
-Initial Volume:	0.25 L
-Flow rate:	0.1 L/min (recirculation)
-Current:	Constant current @ 0.5 A (constant current density)
-Electrolyte:	BDD: 2000 mg/L SO ₄ ⁻ (as NaSO ₄) MMO: 2000 mg/L SO ₄ ⁻ + 200 mg/L Cl ⁻ (as NaCl)

Initial control experiments for each anode were performed without applied current to assess RDX losses throughout the test system, which were found to be <1%.

Duplicate runs with an applied constant current of 0.5 A were then performed with each anode. The current and voltage were monitored throughout the testing. Samples were removed periodically for the following analyses:

- pH (via probe)
- Anions (specifically nitrite and nitrate, as possible end products from RDX degradation)
- RDX and RDX breakdown products MNX, DNX, TNX, and NDAB

As a measure of oxidants generated electrochemically in the test system (e.g., free chlorine, peroxide, ozone), the diethyl-*p*-phenylenediamine (DPD) assay was used. The assay results are presented in this report as free chlorine equivalents, or as the raw absorbance value to represent total oxidants levels. *Note: The DPD method does not provide a measure of hydroxyl radicals due to their extremely short lifetime.*

2.2.2.2 Results and Discussion.

The voltage averaged 7 to 8 volts in all experiments. The average total oxidant detected during the BDD anode experiment was slightly lower than that detected during the MMO anode experiments (~25 vs. ~80 mg/L, expressed as total free chlorine). This likely reflects that the BDD electrolyte solution did not contain chloride, and hence less chlorine-based oxidants were

generated. For the MMO experiments, approximately 50%, 60%, and 70% of the chloride initially present was converted to free chlorine for the SnO₂, RuO₂, and IrO₂ anodes, respectively.

During RDX degradation testing, the pH of the test solution increased for all of the anodes (**Figure 2.2-2**), which was not unexpected with the undivided configuration. The MMO anodes resulted in a fast spike in pH, while the pH during the BDD experiment rose more slowly. Alkaline hydrolysis of RDX is well documented at pH values greater than 10 (9, 14), and slow RDX transformation been observed in slightly alkaline seawater (half-life of several decades) (25). However, the increases in pH observed during these tests were likely not large enough to contribute to significant RDX degradation on its own within the timeframe .

The transformation of RDX in the four experiments is shown in **Figure 2.2-3**. The regressed first order transformation rate constants for RDX in the four experiments are shown in **Table 2.2-1**. The rate constants were similar for all the MMO anodes, with the BDD anode rate a modest 1.2- to 1.5-fold higher than the MMO anode rates. We expected that the BDD system would substantially outperform the MMO systems if oxidative transformation controlled RDX removal. The presence of chloride (and the subsequent generation of oxidized chlorine species) in the MMO experiments was expected to facilitate faster RDX removal. However, the rates of degradation with chloride were not substantially greater than the rates without chloride for the IrO₂ and the RuO₂ anodes (the SnO₂ anode was not tested without chloride).

To prevent the formation of perchlorate, which is known to form via oxidation at BDD anodes, no chloride or oxidized chlorine species were present in the BDD experiments. Additionally, as stated below, the initial cathodic reduction of RDX may have been the rate limiting step. Since all the systems had the same stainless steel cathode, all the rate constants were roughly the same.

None of the known RDX degradation products (MNX, DNX, TNX, NDAB) were detected. Some unidentified peaks were observed in the HPLC chromatograms from both the tests runs with the BDD anode, and in some of the tests runs with the SnO₂ and RuO₂ anodes (example chromatogram in **Figure 2.2-4**), but no additional peaks were observed in any tests with IrO₂ anode.

The degradation of RDX and the production of nitrite (NO₂⁻) and nitrate (NO₃⁻) was also examined in terms of the nitrogen mass balance. As seen in **Figure 2.2-5**, nitrate was produced during the degradation of RDX by all four anodes, but nitrite was only detected in the BDD anode experiments. The moles of nitrite+nitrate reaches a maximum of around 40% of the nitrogen in RDX during the BDD anode experiments, but only reaches around 20% or less of the RDX nitrogen in the MMO anode experiments. This may reflect the more oxidizing conditions in the BDD anode system. It is clear from these data that either both production and degradation of nitrite+nitrate was occurring, or that the missing nitrogen was present in products that were not measured (e.g., nitrous oxide (N₂O), N₂, NH₃, other organic nitrogen).

The coulombic efficiency (CE) for RDX removal is calculated as follows (4):

$$\%CE = \frac{cFVe}{At} 100 \quad \text{Eq. 1}$$

where c is the decrease in the RDX concentration at the end of the experiment (mole/L), F is Faraday's Constant (94,486 C/mole), V is the volume of the batch system (0.25 L), e is the electrons transferred for the initial reduction of RDX [assume 4 (4)], A is the applied current (0.5 A), and t (seconds) is the elapsed time at the end of the experiment. The calculated %CE values are between 7×10^{-2} and 9×10^{-2} percent (Table 2.2-1).

The applied electrical energy per volume for a 50% reduction in RDX concentrations for the 3 MMO electrodes is approximately 45 W-h L^{-1} , compared to an applied energy for a 50% reduction for the BDD electrodes of approximately 30 W-h L^{-1} . These energy requirements are very high, and likely are due to the very low coulombic efficiencies for RDX removal. Operation at low current densities would likely have improved the energy efficiency.

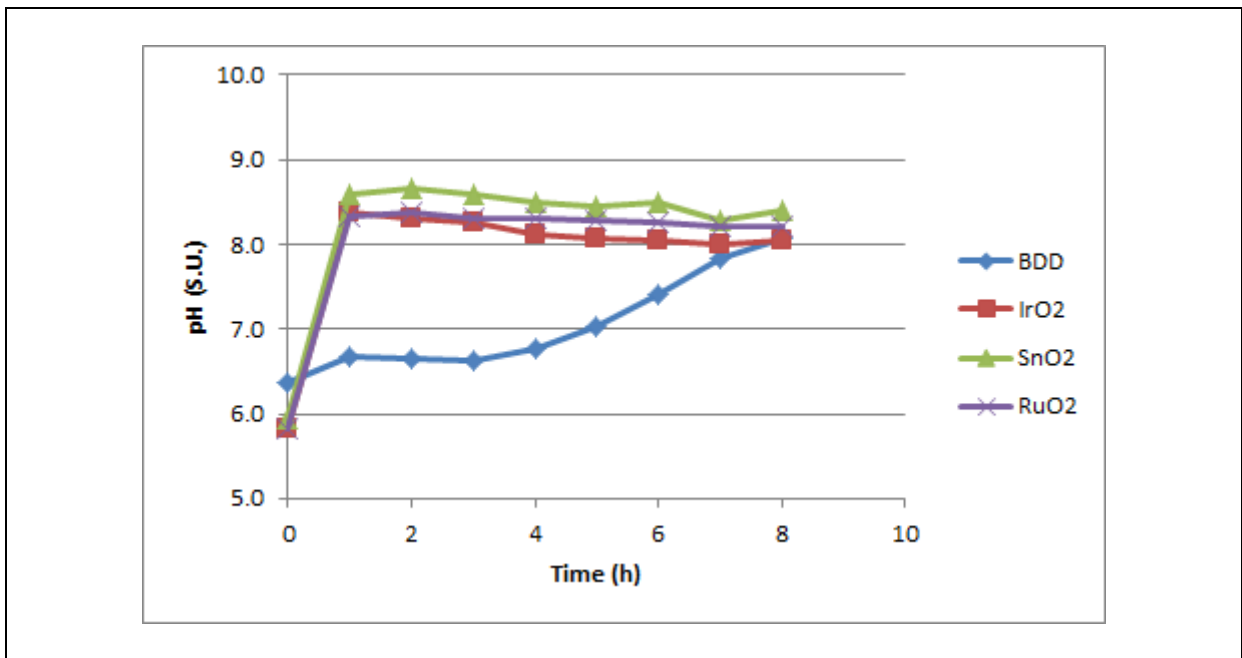


Figure 2.2-2. Average test solution pH over time for the various anodes operated in the undivided cell configuration (n = 2 for each anode).

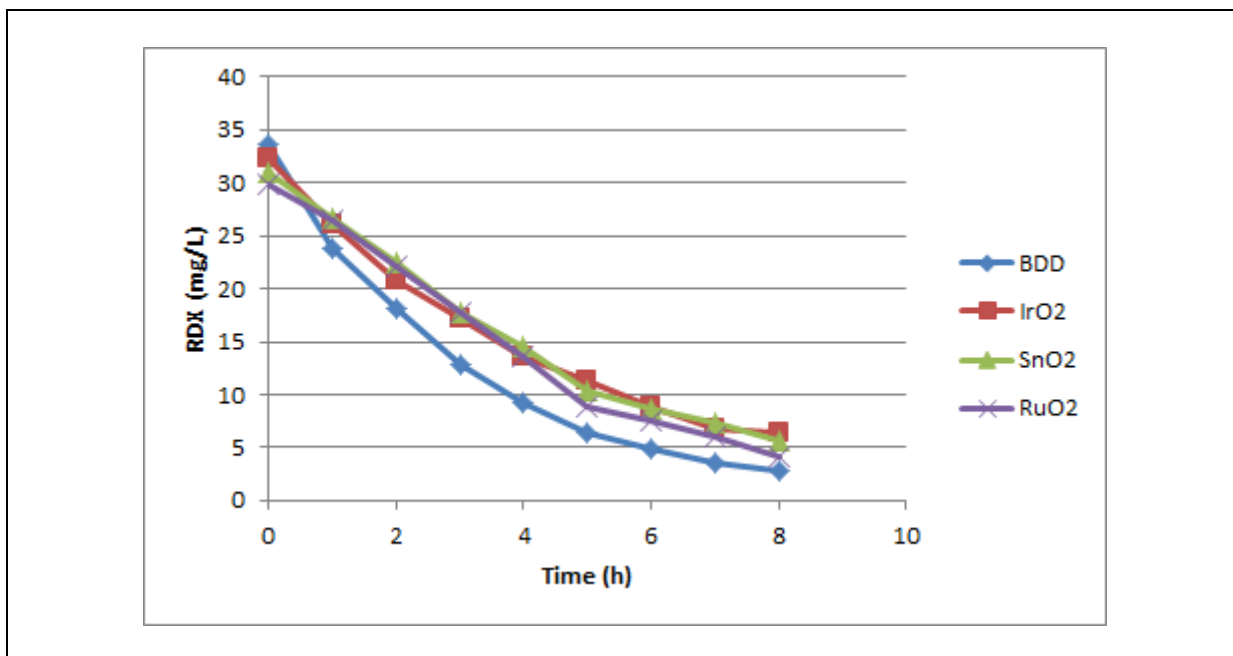


Figure 2.2-3. Degradation of RDX during experiments using the four different anodes (n=2 for each anode).

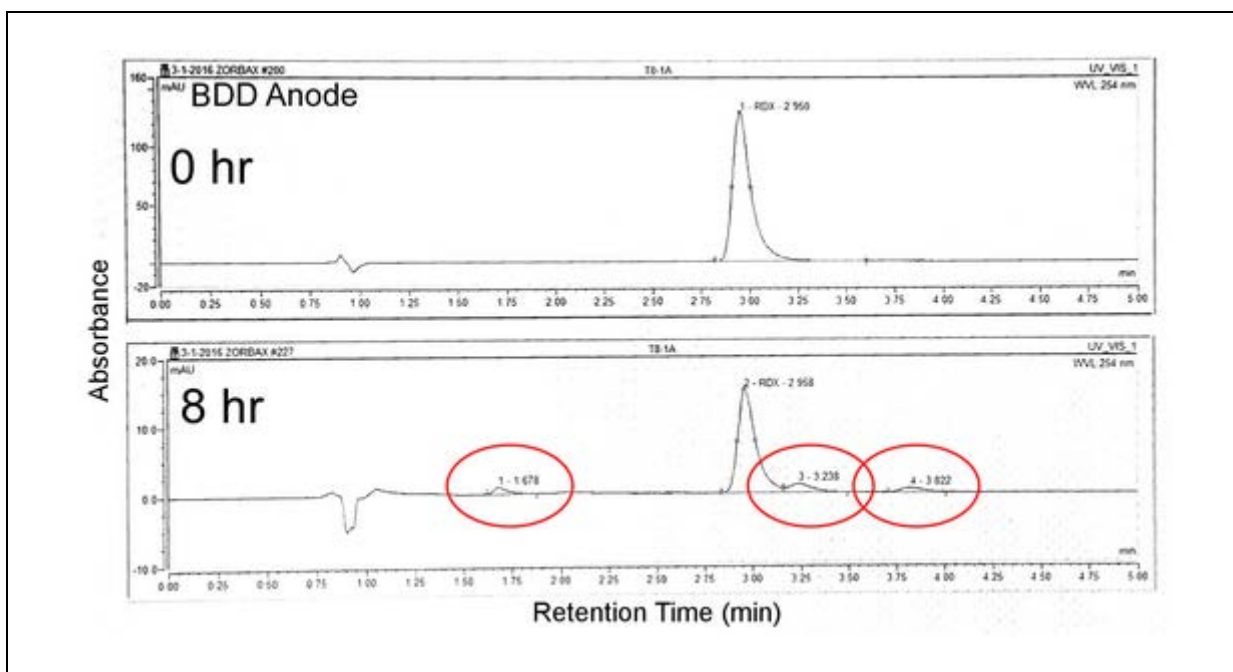


Figure 2.2-4. HPLC chromatogram at 0 hr (top) and 8 hr (bottom) for one of the RDX degradation experiments using the BDD anode showing appearance of unknown peaks (red circles).

	-k (1/h)	± SE	r ²	CE (%)
BDD	0.32	0.01	1.00	0.09
IrO ₂	0.21	0.01	1.00	0.08
IrO ₂ -No Cl	0.22	0.04	0.99	0.06
SnO ₂	0.22	0.02	1.00	0.07
RuO ₂	0.25	0.03	1.00	0.08
RuO ₂ -No Cl	0.20	0.03	0.99	0.07

SE, standard error

Table 2.2-1. Best fit RDX degradation rate coefficients (k; 1/h) and current efficiencies for the four anodes tested.

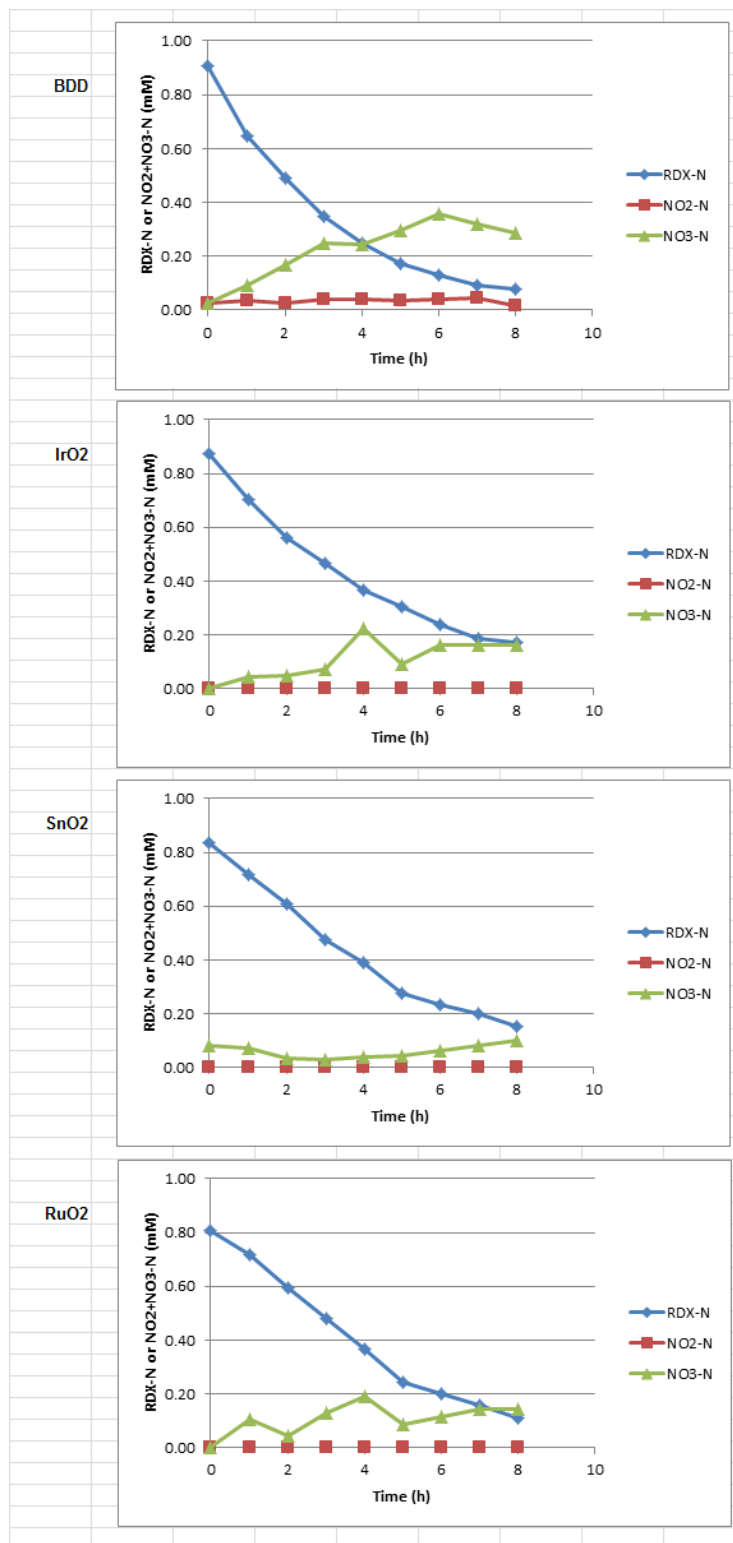


Figure 2.2-5. Changes in RDX, nitrite, and nitrate expressed in mM nitrogen during experiments using the four different anodes (n = 2 for each anode).

2.2.3 Degradation of nitrate and nitrite.

2.2.3.1 Methods.

To investigate the fate of the possible RDX-derived nitrite and nitrate, additional experiments were performed with the BDD and the MMO RuO₂ anodes starting with solutions containing no RDX, but either NaNO₂ or NaNO₃. All other parameters were the same, and chloride was included in the RuO₂ anode test. Changes in nitrate and nitrate were measured over time.

2.2.3.2 Results and Discussion.

The electrochemical degradation of nitrate is already known, with the production of ammonia and/or nitrogen gas, depending on the conditions (10, 16, 19, 28).

During these experiments, both the BDD and the RuO₂ anodes effectively degraded nitrate (**Figure 2.2-7**). The BDD anode generated some nitrite, but it only represented a maximum of ~10% of the initial nitrate added on a molar nitrogen basis, indicating that nitrite was not the terminal breakdown product. Nitrite has been observed as an intermediate during nitrate transformation (19). When nitrite alone was added, it was rapidly oxidized to nitrate, which was then further degraded (**Figure 2.2-8**).

It was also noted that the pH during these experiment also rose rapidly (**Figure 2.2-6**), and reached higher values than observed during the RDX degradation experiments (~10 vs 8.5 S.U.). The exact reasons for this difference are not known, but it could reflect either a higher efficiency of hydroxide formation in the presence of the additional anions, or consumption of hydroxide by RDX and breakdown product reactions in the earlier studies.

These initial results provide proof-of-concept data for electrochemical destruction of dissolved explosive compounds. The observed RDX degradation may represent a two-step process, involving an initial reduction of the RDX at the cathode (analogous to the observed reduction of nitrate to nitrite in these experiments, and previously observed in published literature; (6)). The resulting products were then degraded by the oxidants generated in situ by the system. The intermediate(s) produced via the initial reduction of RDX was either unstable or short lived (e.g., methylenedinitramine (MEDINA), or unable to be detected by the analytical methods employed in this project (e.g., MEDINA, formaldehyde, nitramide).

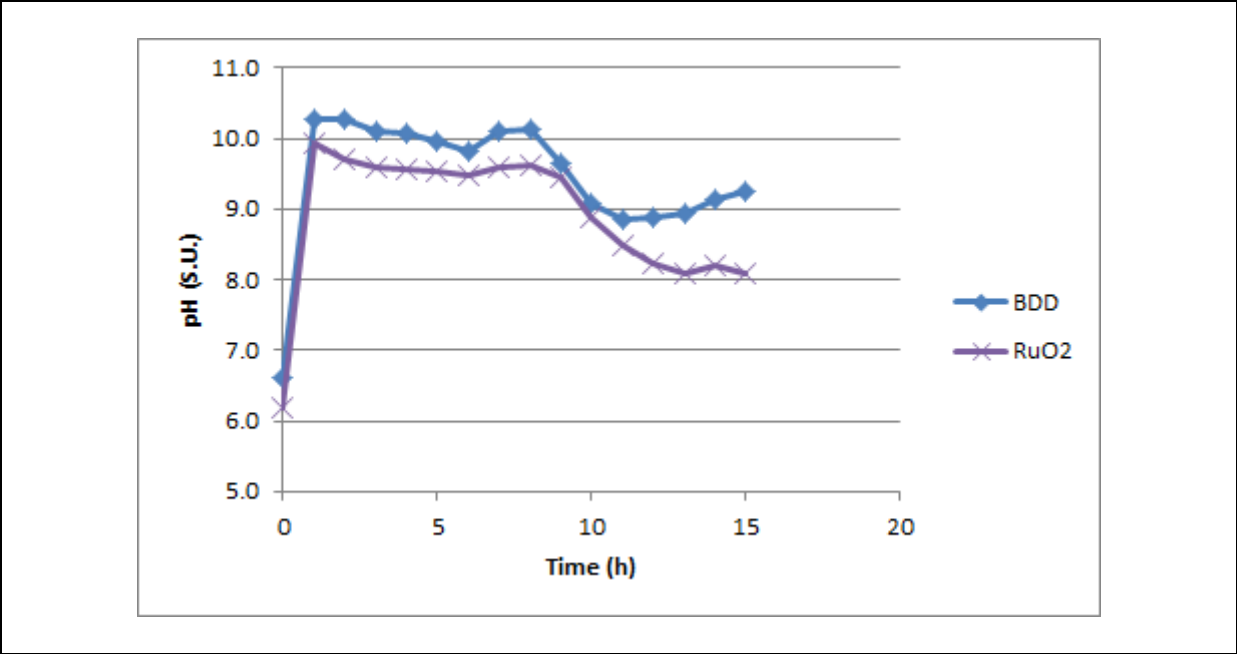


Figure 2.2-6. Changes in the pH of the test solution during degradation of nitrate using the BDD and RuO₂ anodes.

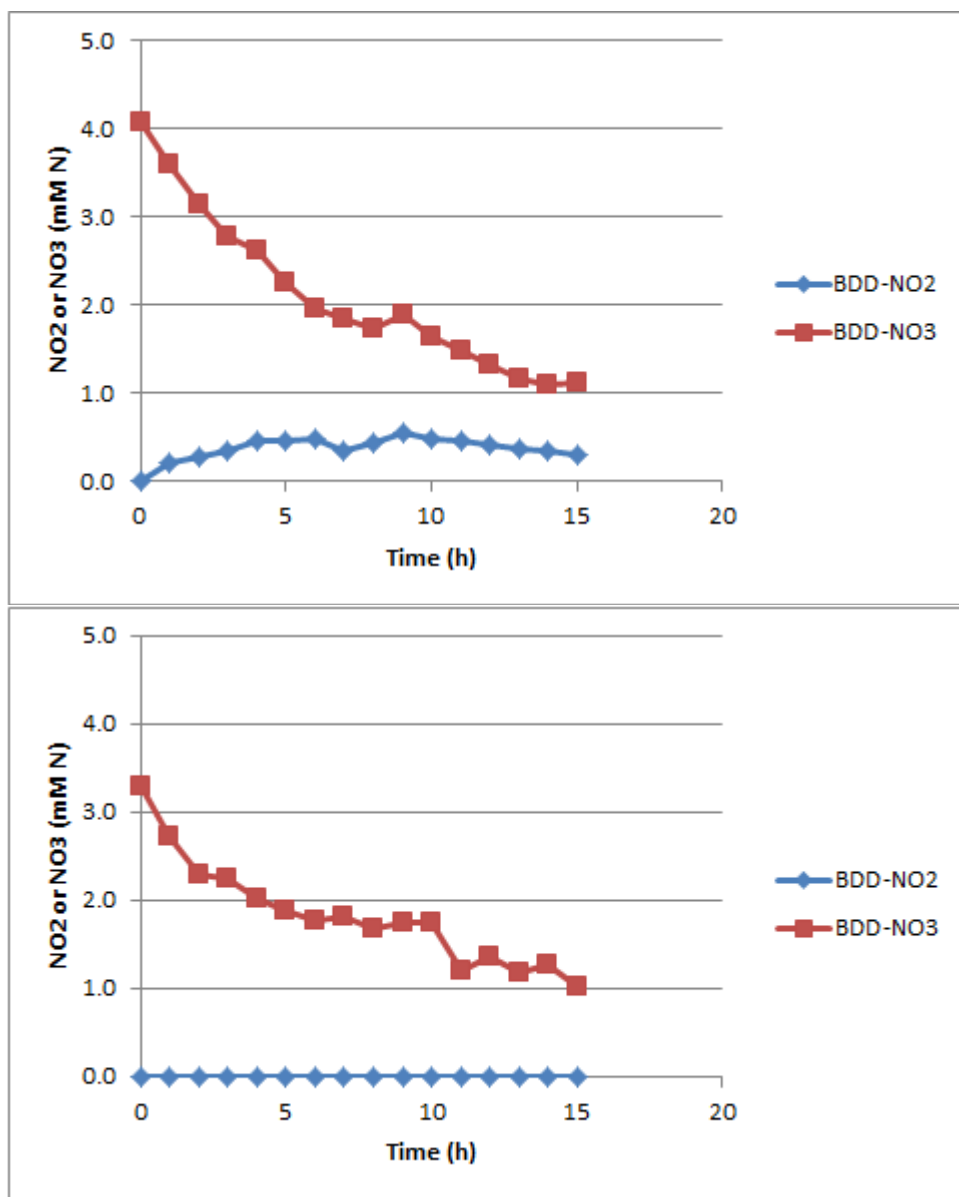


Figure 2.2-7. Degradation of nitrate and production of nitrite during experiments using the BDD and RuO₂ anodes.

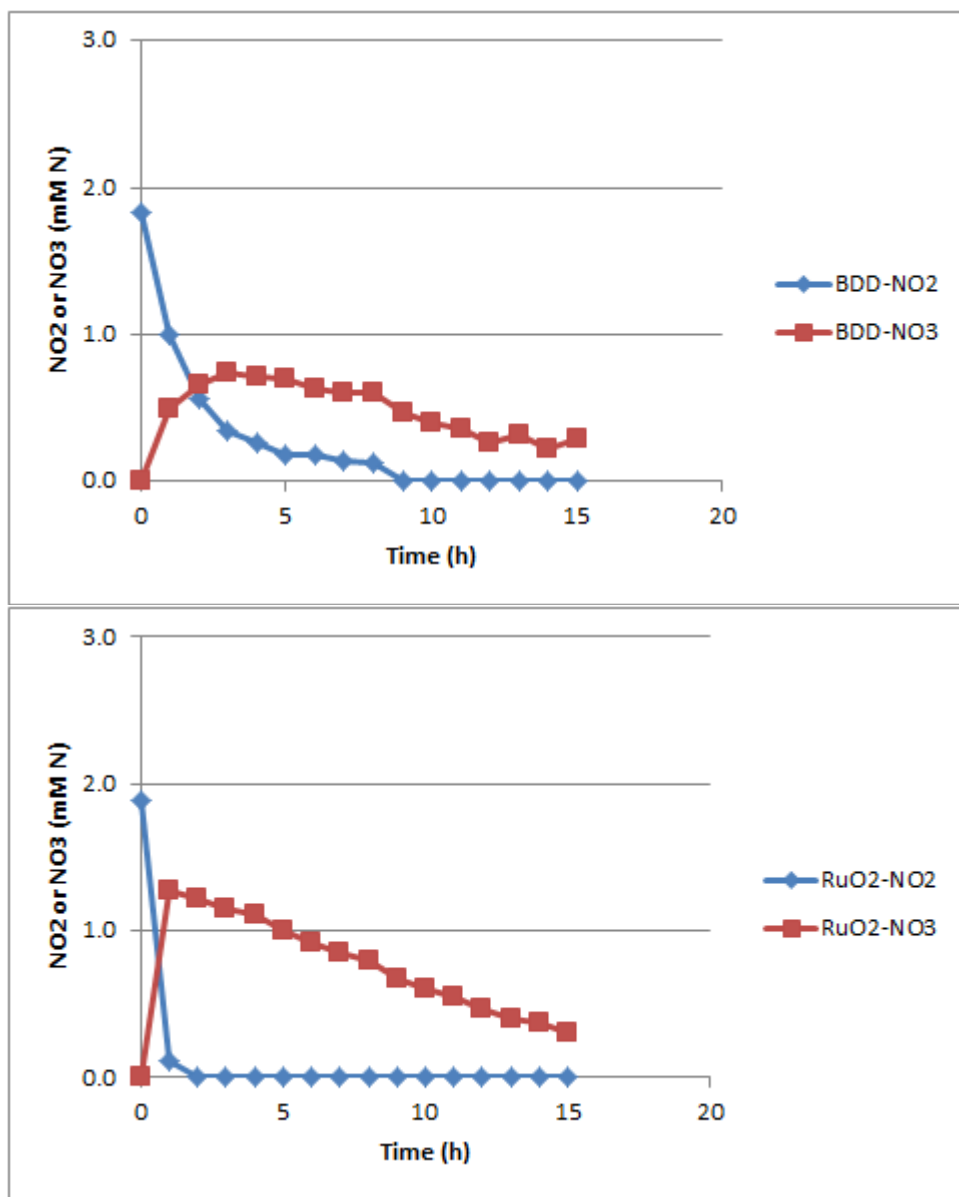


Figure 2.2-8. Degradation of nitrite and production of nitrate during experiments using the BDD and RuO₂ anodes.

2.2.4 Effect of electrolyte concentration and flow rate on RDX degradation.

2.2.4.1 Methods.

It was decided to continue testing with the BDD anode, which evidenced the greatest RDX degradation rates, and the IrO₂ anode, which evidenced the smallest production of residual nitrite+nitrate and no evidence of unknown HPLC peaks. These two anodes were coupled with stainless steel cathodes for this testing.

Based on the proof-of-concept data, efforts were then focused on examining how various parameters influence the RDX degradation kinetics as follows:

- a) Effect of flow rate. The standard flow rate during the initial testing was 0.1 L/min. During these experiments, RDX degradation was tested at flow rates of 0.05 L/min (50% initial) and 0.2 L/min (200% initial). The different flow rates were used to determine the effects of the increased flow velocity on the observed rate of RDX degradation and breakdown product generation, as well as attempt to provide insight into whether RDX degradation was controlled by external mass transfer, or current controlled on the electrode surface.
- b) Effect of electrolyte concentration. The standard electrolyte during the initial testing was 2000 mg/L sodium sulfate (as sulfate). During these experiments, RDX degradation was tested using 1000 mg/L (50% initial) and 200 mg/L (10% initial) sodium sulfate; no chloride was added to the solution. The lower sulfate concentrations would be desirable in future full-scale implementation as they could lower operation and waste disposal costs. It is recognized that changing the electrolyte solution results in a change in its electrical conductivity, and thus a change in the applied voltage needed to attain the selected current density. Such changes in the applied voltage could impact surface reactions on the electrodes.

Standard analytical methods for RDX, breakdown products (NDAB, NX's), and anions (nitrite, nitrate) were as described above.

2.2.4.2 Results and Discussion.

Results are summarized in **Table 2.2-2**. In all experiments, sulfate concentrations remained unchanged during electrochemical treatment, indicating that the sulfate was essentially inert in solution (consistent with our and other's previous studies, e.g., ref (33)).

Overall, no significant changes in RDX transformation rates were observed with either the BDD or the IrO₂ system in response to the flow rate changes. This would indicate that the reactions are current dependent, as opposed to bulk mass transfer dependent.

Decreasing the sulfate concentration with the BDD electrode resulted in approximately 20% higher RDX degradation rates, with 4-fold higher voltage and a decrease in pH of 1 S.U. In contrast, with the IrO₂ electrode, decreasing the sulfate concentration from 2000 mg/L to 200 mg/L did not result

in any significant change in the RDX degradation rate, even with a 4-fold maximum voltage increase and a maximum pH increase of 1 S.U. One plausible explanation for this difference in behavior between the electrode materials with respect to RDX transformation is based on oxidant generation. DPD levels for the BDD anode increase with increasing voltage (decreasing electrolyte), while DPD levels for the MMO anode are not impacted by the voltage. Thus, the elevated voltage may have facilitated oxidant generation at the BDD anode surface, resulting in slightly enhanced RDX transformation.

The mass balance of RDX nitrogen (molar basis) recovered as nitrite plus nitrate increased in the BDD system as the sulfate concentration was reduced, reaching 96% at 200 mg/L sulfate. As it was previously demonstrated that nitrite and nitrate are degraded in the BDD system with 2000 mg/L sulfate, these results would seem to imply that the lower sulfate concentration resulted in less degradation of nitrogen released from RDX during the degradation process. In the IrO₂ system, very small amounts of nitrite and nitrate were detected under all the test conditions (0 to 6%, indicating that their destruction is not affected by the sulfate concentration). The key difference between the BDD and IrO₂ systems appears to be the oxidant levels (based on the DPD values), indicating that elevated oxidant formation leads to higher nitrite plus nitrate accumulation as RDX degrades.

For the undivided cell configuration, the RDX breakdown product 4-nitro-2,4-diazabutanal (NDAB) was sporadically detected at low concentrations (usually much below 0.05 mg/L), and the nitroso-containing breakdown products hexahydro-1-nitroso-3,5-dinitro-1,3,5-triazine (MNX), hexahydro-1,3-dinitroso-5-nitro-triazine (DNX), and hexahydro-1,3,5-trinitroso-1,3,5-triazine (TNX) were not detected above the detection limit of 0.05 mg/L.

Anode	Cathode	Flow Rate (L/min)	Na ₂ SO ₄ Electrolyte (mg/L)	Maximum Voltage (V)	Maximum pH (S.U.)	Maximum DPD Oxidant (absorbance)	RDX Degradation Rate			Rate Relative to Standard Parameters ¹	Recovery of NO ₂ +NO ₃ Relative to Initial	
							-k (1/h)	±SE	r ²		RDX (mM-N)	CE (%)
BDD	SS	0.10	2000	7	8.1	0.48	0.32	0.01	1.00	100	0.32	0.09
			1000	10	9.8	0.51	0.38	0.01	1.00	120	0.67	0.08
			200	26	7.0	0.54	0.38	0.03	0.99	121	0.96	0.07
		0.05	200	22	8.2	0.58	0.41	0.02	1.00	131	0.62	0.08
		0.20	200	26	8.4	0.44	0.38	0.01	1.00	122	0.59	0.08
IrO ₂	SS	0.10	2000	7	8.0	0.03	0.21	0.01	1.00	100	0.06	0.06
			1000	10	8.9	0.03	0.22	0.02	1.00	102	0.05	0.06
			200	26	8.9	0.03	0.22	0.04	0.99	104	0.06	0.06
		0.05	200	22	9.6	0.02	0.19	0.03	0.99	88	0.00	0.06
		0.20	200	26	9.3	0.03	0.24	0.05	0.99	114	0.00	0.07

¹ "Standard Parameters" defined as 2000 mg/L sulfate electrolyte and flow rate of 0.10 L/min (highlighted gray above).

Table 2.2-2. Effects of electrolyte concentration and flow rate on RDX degradation with the BDD and IrO₂ anodes in the undivided cell configuration.

2.3 Task 3 – Degradation of RDX in divided cell configuration

2.3.1 Goal and Introduction

In light of the overall project goal

To evaluate which electrochemical designs would be effective for explosive and propellant treatment with respect to specific anodes and cell configurations.

The focus of this task was to evaluate the degradation of RDX in the divided cell configuration, in which the anolyte and catholyte are circulated in separated loops. An illustration of this configuration is presented in **Figure 2.3-1**. Both cathodic and anodic degradation using the BDD and IrO₂ anodes couple with SS cathodes was examined.

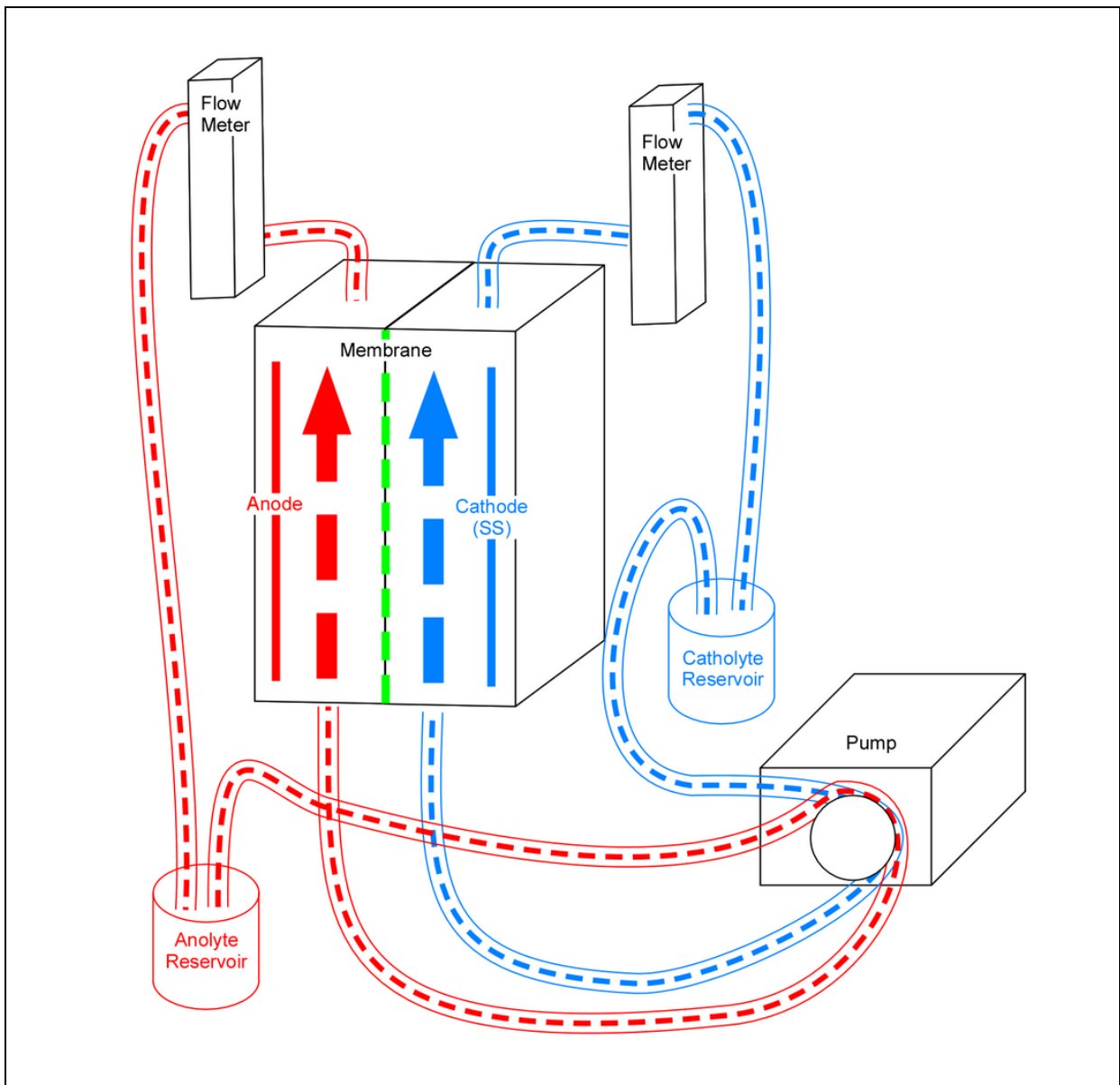


Figure 2.3-1. Illustration of the divided cell configuration.

2.3.2 RDX degradation at constant current

2.3.2.1 Methods.

Initial conditions for the divided cell configuration testing were as follows:

-Configuration:	Divided flow cell
-RDX:	Approximately 30 to 40 mg/L
-Cathode:	SS
-Membrane:	DuPont Nafion® 117 (cation exchange membrane, 0.17 mm thickness)
-Gap:	8 mm (distance between anode and cathode)
-Electrode Area:	10 cm ²
-Initial Volume:	0.25 L
-Flow rate:	0.1 L/min (recirculation in both anode and cathode loops)
-Current:	Constant current @ 0.5 A (constant current density)
-Electrolyte:	1000 mg/L SO ₄ ⁻ (as NaSO ₄)

Both anodic and cathodic RDX degradation was examined, The final molarity of acid (as HCl) and alkali (as NaOH) the anolyte and catholyte solutions, respectively, were also determined via titration against standard solutions of 1 N HCl or NaOH.

2.3.2.2 Results and Discussion.

The results are summarized in **Table 2.3-1**, which also includes the representative results from the undivided cell configuration testing for comparison. RDX degradation in the BDD system was observed in both the catholyte (stainless steel cathode) and the anolyte (BDD anode) solutions, demonstrating that both a reductive (cathode) and oxidative (anode) RDX transformation pathways occurs in the BDD/SS electrode system. Cathodic degradation was approximately 20% higher than observed in the undivided cell configuration with 1000 mg/L sulfate, while anodic degradation was about 15% lower than that observed in the undivided system. Greater RDX degradation was also observed in the catholyte solution of IrO₂ system (approximately 60% higher rate), but minimal anodic degradation was observed.

It should be noted that during the initial experiments with the divided cell configuration, it was noticed that relatively high NDAB concentrations were detected in the catholyte solution samples, a known product of alkaline hydrolysis of RDX (3) While the RDX analyses were performed in almost real time, the NDAB analyses were often performed several days after the samples were collected. Because the catholyte had an elevated pH (>11), continued alkaline hydrolysis of the RDX occurred in the sample vial, leading to elevated NDAB concentrations. Therefore, a supplemental RDX degradation experiment was performed with the BDD system during which duplicate subsamples were collected, one of which was brought to approximately pH 7 by mixed 0.5 mL of sample with 0.5 mL of 1 M phosphate buffer (K₂HPO₄-3H₂O, 170 g/L; KH₂PO₄-H₂O,

40 g/L; pH 7.3) immediately after collection. The results are shown in **Figure 2.3-2**. Adjusting the pH resulted in a slight decrease in the calculated RDX degradation rate coefficient. More importantly, buffering dramatically lowered the apparent NDAB formation during the time between sample collection and analysis. After this determination, subsequent cathodic RDX degradation experiments included pH neutralization for samples analyzed for RDX and NDAB. Buffering would also be warranted during anodic RDX degradation, as low pH has been demonstrated to lead to NDAB degradation as well (26).

For both the BDD and the IrO₂ systems, very low recovery of RDX-derived nitrogen was observed during cathodic degradation (3 and 5%, respectively). However, anodic RDX degradation with the BDD system resulted in 48% of the nitrogen recovered as nitrite and nitrate, which was about 20% lower than with the undivided cell configuration with the same sulfate concentration. As with the BDD undivided cell configuration results, it is believed that the higher radical concentration observed in the anodic BDD treatment (reflected in the higher DPD assay values) was the cause of the higher concentrations of nitrite and nitrate RDX transformation products.

The nitroso-containing breakdown products MNX, DNX, and TNX were not detected above the detection limit of 0.05 mg/L. NDAB, a known breakdown product of RDX under alkaline conditions (3), appeared to be produced then degraded in the catholyte solution during cathodic RDX degradation in the both the BDD and IrO₂ systems, whereas no NDAB was detected during anodic degradation in the BDD system.

The applied electrical energy per volume for a 50% reduction in RDX concentrations for the IrO₂ electrode, assuming treatment would involve sequential (cathodic-anodic or anodic-cathodic) electrolysis is approximately 38 W-h L⁻¹. This is slightly less than the 45 W-h L⁻¹ observed in the undivided cell configuration, and is likely due to mitigation of anodic scavenging reactions in the divided cell. In comparison, the applied energy for a 50% reduction for the BDD electrodes (again, assuming treatment would have occurred using sequential anodic-cathodic or cathodic-anodic electrolysis) was approximately 20 W-h L⁻¹, which is 33% less than the energy demand needed for comparable RDX removal in the undivided cell.

For the BDD anodes, treatment was observed in both the catholyte and anolyte, which improved the overall efficiency of the treatment process. While these energy values are still quite high (due to coulombic efficiencies that remain well below 1%), results suggest that treatment using a divided cell configuration shows promise for improved energy efficiency, especially when using BDD anodes. As discussed in the following section, operating at much lower applied current and voltage would likely serve as a means to further reduce the energy demand.

Anode	Cathode	Configuration	RDX in Catholyte or Anolyte	Flow Rate (L/min)	Na ₂ SO ₄ Electrolyte (mg/L)	Maximum Voltage (V)	Final pH (S.U.)	RDX Degradation Rate			Recovery of NO ₂ +NO ₃ Relative to Initial RDX (mM-N)	CE (%)	
								Maximum DPD Oxidant (absorbance)	-k (1/h)	±SE			r ²
BDD	SS	Undivided	N/A	0.10	1000	10	9.8	0.51	0.38	0.01	1.00	0.67	0.08
IrO ₂	SS	Undivided	N/A	0.10	1000	10	8.9	0.03	0.22	0.02	1.00	0.05	0.06
BDD	SS	Divided	Catholyte	0.10	1000	10	11.4	0.05	0.45	0.03	1.00	0.05	0.09
			Anolyte	0.10	1000	10	2.3	0.47	0.26	0.02	0.99	0.48	0.09
IrO ₂	SS	Divided	Catholyte	0.10	1000	10	11.4	0.04	0.36	0.06	0.99	0.05	0.08
			Anolyte	0.10	1000	10	2.3	0.19	0.00	0.00	0.67	0.00	0.00

Table 2.3-1. Anodic and cathodic RDX degradation with the BDD and IrO₂ systems in the divided cell configuration.

Data from the undivided cell configuration are presented for comparison.

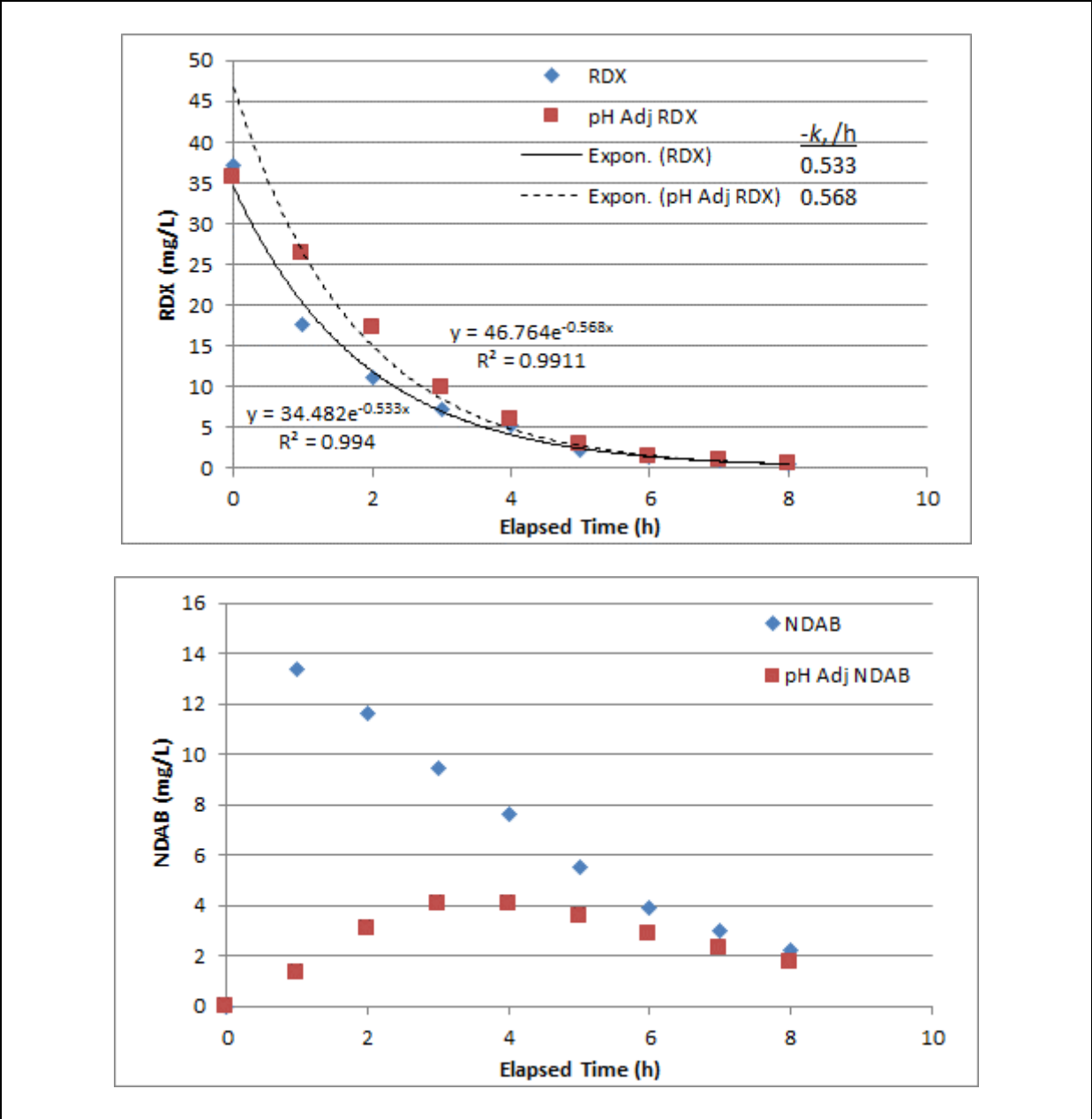


Figure 2.3-2. Effect of pH neutralization at time of sample collection on the calculated cathodic RDX degradation rate coefficient (top) and NDAB formation (bottom) in the BDD system.

2.4 Task 4 – Degradation of nitrocellulose in divided cell configuration

2.4.1 Goal and Introduction

In light of the overall project goal

To evaluate which electrochemical designs would be effective for explosive and propellant treatment with respect to specific anodes and cell configurations.

The focus of this task was to demonstrate cathodic degradation of solid nitrocellulose (NC).

2.4.2 System retrofit.

To avoid any possible incompatibility issues flowing from the extreme low and high pH values in the anodic and cathodic loops, the system was retrofitted using only teflon lined tubing (Tygon SE-200, Saint-Gobain, P/N:AJD00017), except for norprene tubing in the peristaltic pump head. Quick-release fittings were installed, and an in-line strainer unit (200 mesh polyethylene strainer cup, polypropylene and polystyrene casing, ~30 ml liquid or 1.5 g solid capacity inside the cup) was placed in the cathodic loop to hold solid nitrocellulose. An illustration of the cathodic half-cell is shown in **Figure 2.4-1**, and photos of the retrofitted system are shown in **Figure 2.4-2**.

2.4.3 Nitrocellulose analysis

2.4.3.1 Methods.

In order to effectively assess the electrochemical degradation of nitrocellulose (NC), efforts were directed at optimizing methods for determination of the percent nitrogen (%N) in nitrocellulose.

To assist in optimizing the %N analysis, nitrocellulose with a certified nitrogen content was special ordered from Ladd Research Industries (Williston, VT). The material obtained contained 12.0% nitrogen on a dry weight basis based on the manufacturer's data.

The method for %N determination was based on published methods (13, 22, 23), and consisted of digestion/denitration of the NC sample in 5 N NaOH for 10 minutes at approximately 100°C, followed by dilution and measurement of the nitrite and nitrate released into the solution using ion chromatography. A control consisting of NC in water only was used to account for free nitrogen species.

The method was applied to the certified NC, as well as to samples of NC fines waste supplied to us via Picatinny Arsenal.

2.4.3.2 Results and Discussion.

Analysis of the certified 12.0% N NC material yielded calculated %N ranging from 10.99 to 12.46 %N (or 90 to 104% of the certified value).

The NC fines waste yield initial %N ranging from 11.88 to 12.26%.

The preliminary results indicates that the %N analytical method yielded relatively accurate and reproducible results.

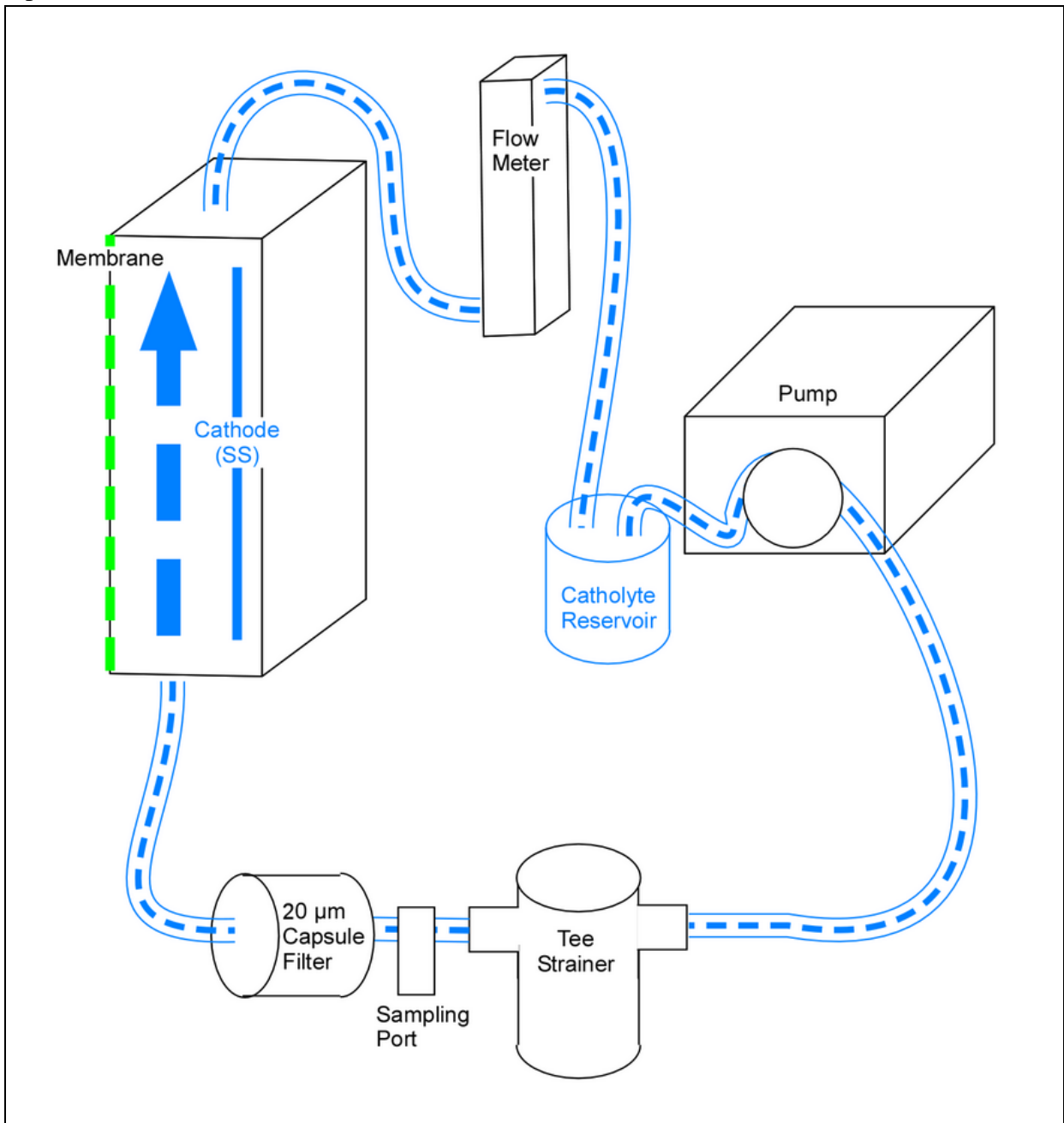


Figure 2.4-1. Illustration of the retrofitted electrochemical test system.
(Note: Only the cathodic half-cell is represented.)

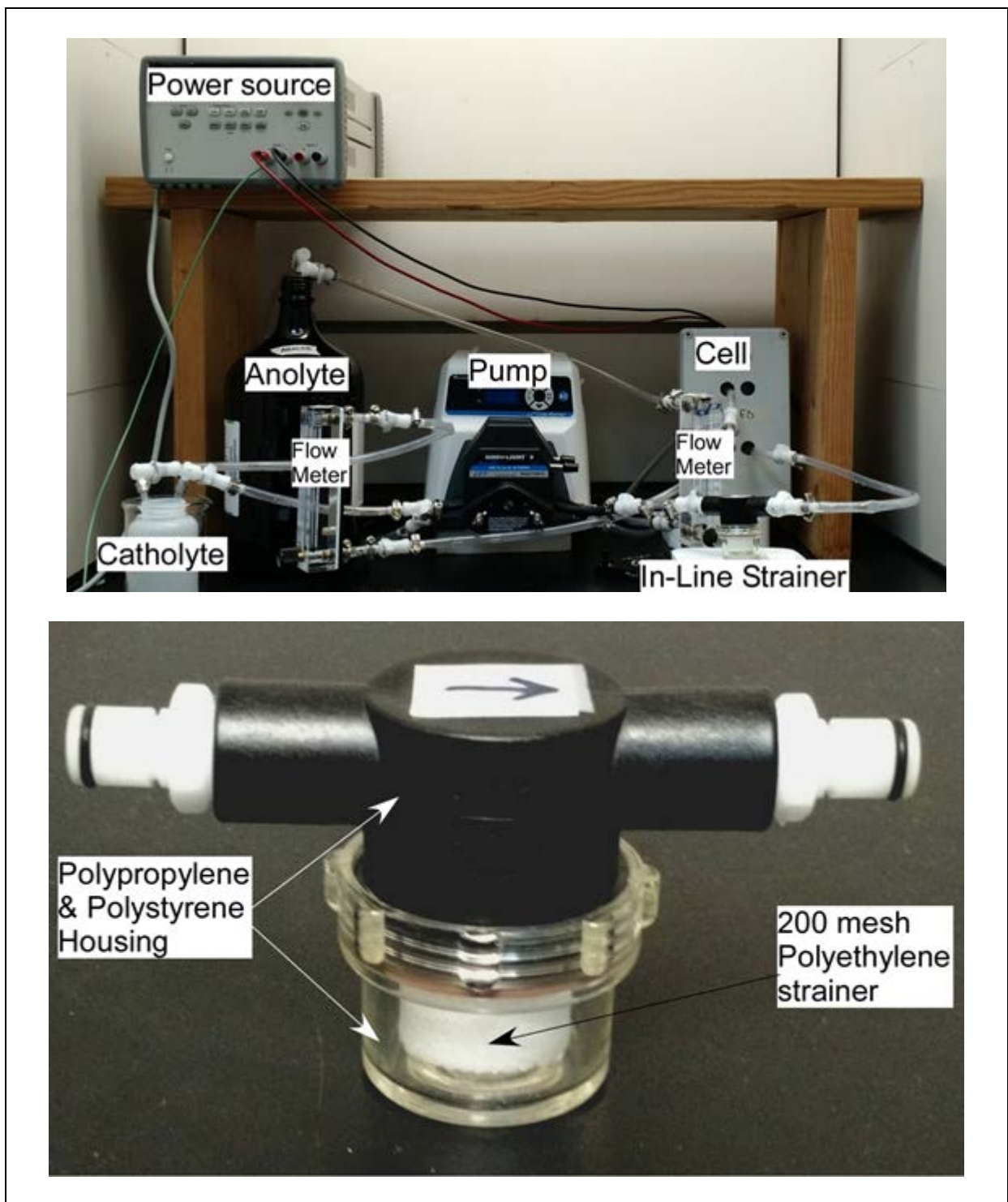


Figure 2.4-2. Photographs of the retrofitted electrochemical system (top) and the in-line strainer (bottom).

2.4.4 Bulk hydrolysis of NC fines

2.4.4.1 Methods.

A simple test was performed to assess the rate and extent of NC fines hydrolysis with various initial hydroxide concentrations. Two grams (dry weight) of NC fines were added to solutions of 0.05, 0.1 and 0.5 N NaOH. The solution was mixed at 500 rpm at room temperature, and samples were removed periodically and analyzed for nitrate and nitrate.

2.4.4.2 Results and Discussion.

Batch NC hydrolysis results are shown in **Figure 2.4-3**. As expected, the NC degradation rate was proportional to hydroxide concentration. Hydroxide in the 0.3 to 0.4 N range are expected to be achievable using the electrochemical system. Additionally, previous literature indicates that increasing the reaction temperature should increase denitration reaction rates (32). While not examined during these experiments, operating the electrochemical system at an elevated temperature may be an avenue to explore during later optimization efforts.

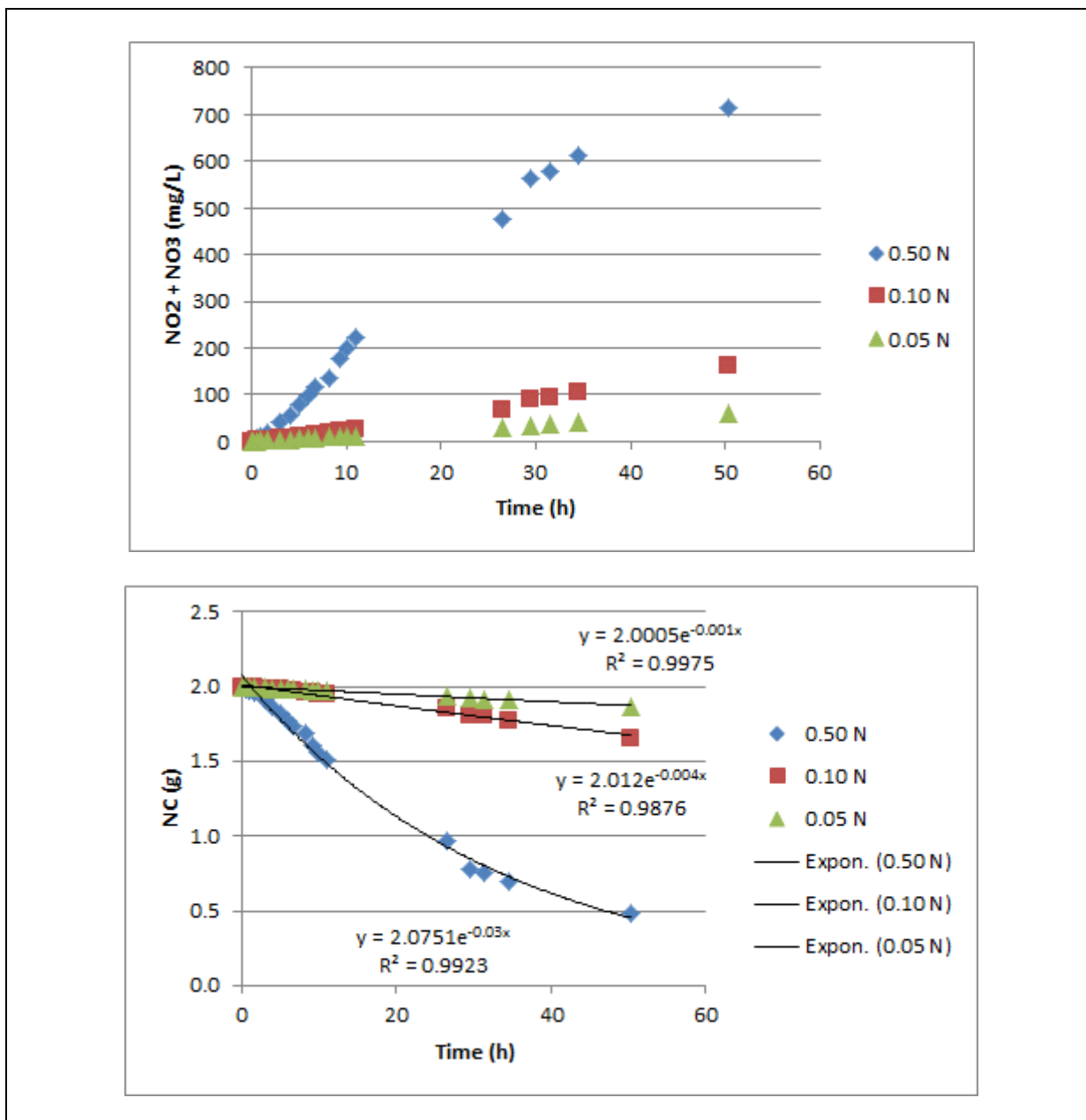


Figure 2.4-3. Production of nitrite and nitrate (top) and calculated NC degradation rates (bottom) during batch alkaline hydrolysis of NC with three different initial hydroxide concentrations.

2.4.5 Determination of minimum voltage to generate steady current

2.4.5.1 Methods.

Up to this point, all electrochemical experiments had been performed under constant current conditions. However, to be power efficient, and to avoid undesirable side reactions, the voltage of the electrochemical system must be set to the minimum which overcomes the inherent resistance of the electrode/electrolyte, while allowing the desired reaction(s) to occur. In our system targeting

alkaline hydrolysis, the reaction of interest was water electrolysis, which accounts for most of the faradaic current in the system at lower voltages. As such, the voltage needed to be set to allow for a reasonable hydroxide generation rates, while avoiding reduction of the sodium or other undesirable side reactions (i.e., at higher voltages), which could lead to fouling of the cathode or damage to the Nafion membrane dividing the cells.

To examine this, a sequential series of three voltage vs. current tests were performed with both the boron doped diamond (BDD) and IrO₂ electrode systems. The anolyte for this testing was 2.5 L of 5000 mg/L sulfate and the catholyte was 0.25 L of 1000 mg/L sulfate, and the flow rate through both loops was 0.1 L/min. Each test started at zero volts, which was increased in increments (0.2 V) up to a maximum of 8 V. The resulting current after each incremental voltage was recorded after five seconds of stabilization. The testing was performed three times for each anode. Voltage (y-axis) vs. current (x-axis) was plotted, and a linear interpolation was performed to find the y-intercept.

2.4.5.2 Results and Discussion.

As seen in **Figure 2.4-4**, the applied voltage for electrolysis (as indicated as y-intercept) using the BDD anode was approximately 3 V, while that for the IrO₂ was 2.5 V. The changes in the slopes of voltage vs. current plots are assumed to reflect the changes in the conductivity of the electrolyte solution due to sodium transport and hydroxide formation (as evidenced by increased pH of the catholyte). These changes likely increased the ionic strength of the electrolyte, thereby reducing the resistance and causing the slope of the voltage vs. current line to decrease (e.g., lower applied voltage required to achieve a given current).

The literature indicates that the standard reduction potential for sodium is approximately -2.7 V relative to hydrogen (1). This information, combined with our testing results, indicated that further experiments should be performed under a constant voltage of 4 V, thereby minimizing the reduction of sodium ions, resulting in plating out of elemental sodium.

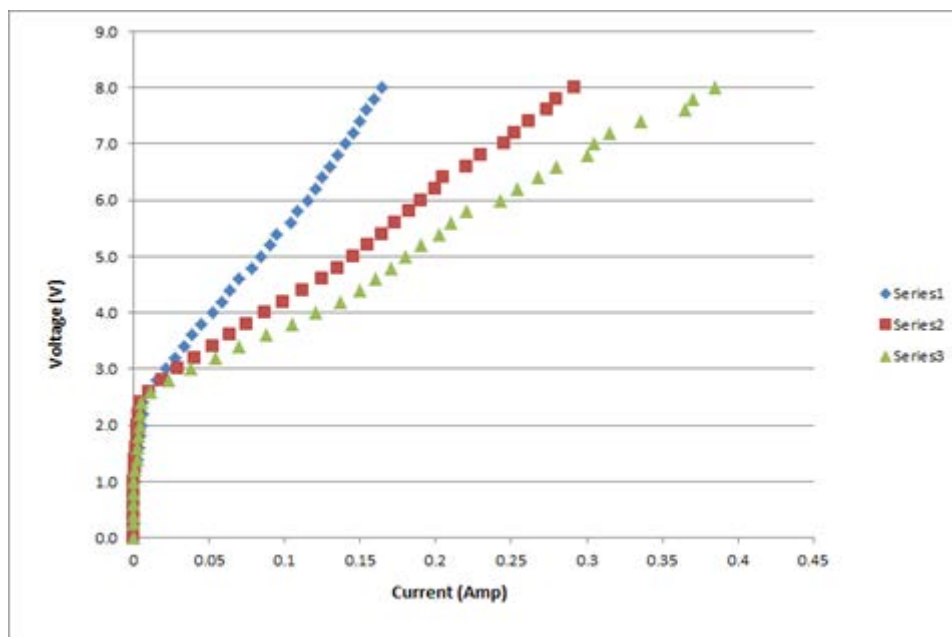
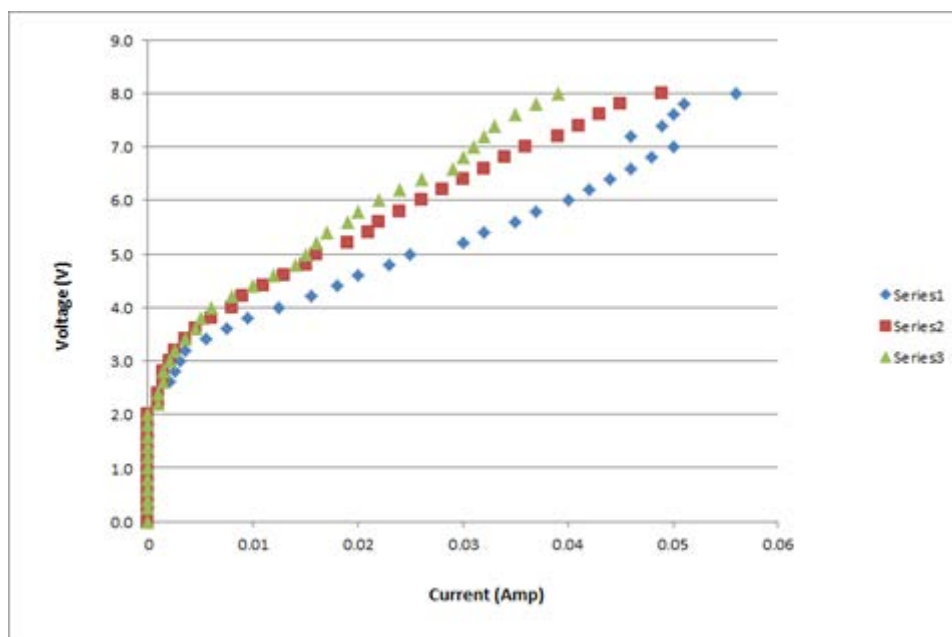


Figure 2.4-4. Plots of voltage vs. current in the BDD electrode system (top) and the IrO₂ electrode system (bottom).

2.4.6 Cathodic production of hydroxide

2.4.6.1 Methods.

The Nafion membrane used in the divided electrochemical cell experiments is much more permeable to cations than anions. As sodium ions move from the anolyte to the catholyte, cathodic reactions and charge balance requirements result in increased concentrations of hydroxide in the catholyte and the pH of the catholyte thus increases. Thus, while evaluating both the BDD and IrO₂ electrode systems cathodic production of hydroxide, the sodium sulfate concentration and/or the volume of the anolyte was sequentially increased.

2.4.6.2 Results and Discussion.

Under the standard conditions of 250 ml of 1000 mg/L sulfate for both anolyte and catholyte, and a constant current of 0.5 A, both the BDD and the IrO₂ systems generated a catholyte hydroxide concentration of approximately 0.02 N in 8 h.

For the BDD, increasing the anolyte sulfate to 10000 and 50000 mg/L (current = 0.5 A) resulted in catholyte hydroxide concentrations of 0.1 and 0.2 N, respectively, in 4 h. Running the system for 24 h with the highest anolyte sulfate concentration, but at a slightly lower current of 0.2 A yielded 0.5 N hydroxide in the catholyte. However, the very high anolyte sulfate concentrations resulted in deterioration of the Nafion membrane (37), and possible damage to the BDD anode (18), as indicated by visual inspection of the cell components. This was speculated to be the result of the production of persulfates in the acidic anolyte (not directly measured). This was also under constant current conditions, which resulted in voltages greater than 4 V.

The IrO₂ system was further tested using 2.5 L of 5000 mg/L sulfate as the anolyte, paired with the standard 250 ml of 1000 mg/L sulfate for the catholyte. At a constant voltage of 4 V, the catholyte hydroxide averaged 0.1 N within 8 h, and up to 0.4 N after 2.5 days of operation, with no apparent damage to the electrodes or membrane.

These results indicated that the NC hydrolysis was feasible using the IrO₂ system to cathodically generate hydroxide.

2.4.7 Cathodic degradation of nitrite and nitrate

2.4.7.1 Methods.

Prior to initiating NC degradation testing, the IrO₂ system was evaluated to determine how quickly any nitrite and nitrate liberated during NC hydrolysis would be degraded in the catholyte. The IrO₂ system was prepared using 2.5 L of 5000 mg/L sulfate as the anolyte, paired with the standard 250 ml of 1000 mg/L sulfate for the catholyte, and the catholyte was spiked with either sodium nitrite or sodium nitrate (nominal concentrations of 20 mg/L). The system was operated at a constant voltage of 4 V.

2.4.7.2 Results and Discussion.

As seen in **Figure 2.4-5**, both nitrite and nitrate undergo cathodic degradation, with some nitrite produced as a nitrate reductive transformation product. These experiments provided nitrite and nitrate degradation (and production) rates which were subsequently used to correct the observed nitrate and nitrite concentrations detected during NC hydrolysis experiments. This allowed a more accurate measurement of overall NC denitration extent, and improved the calculated nitrogen mass balances.

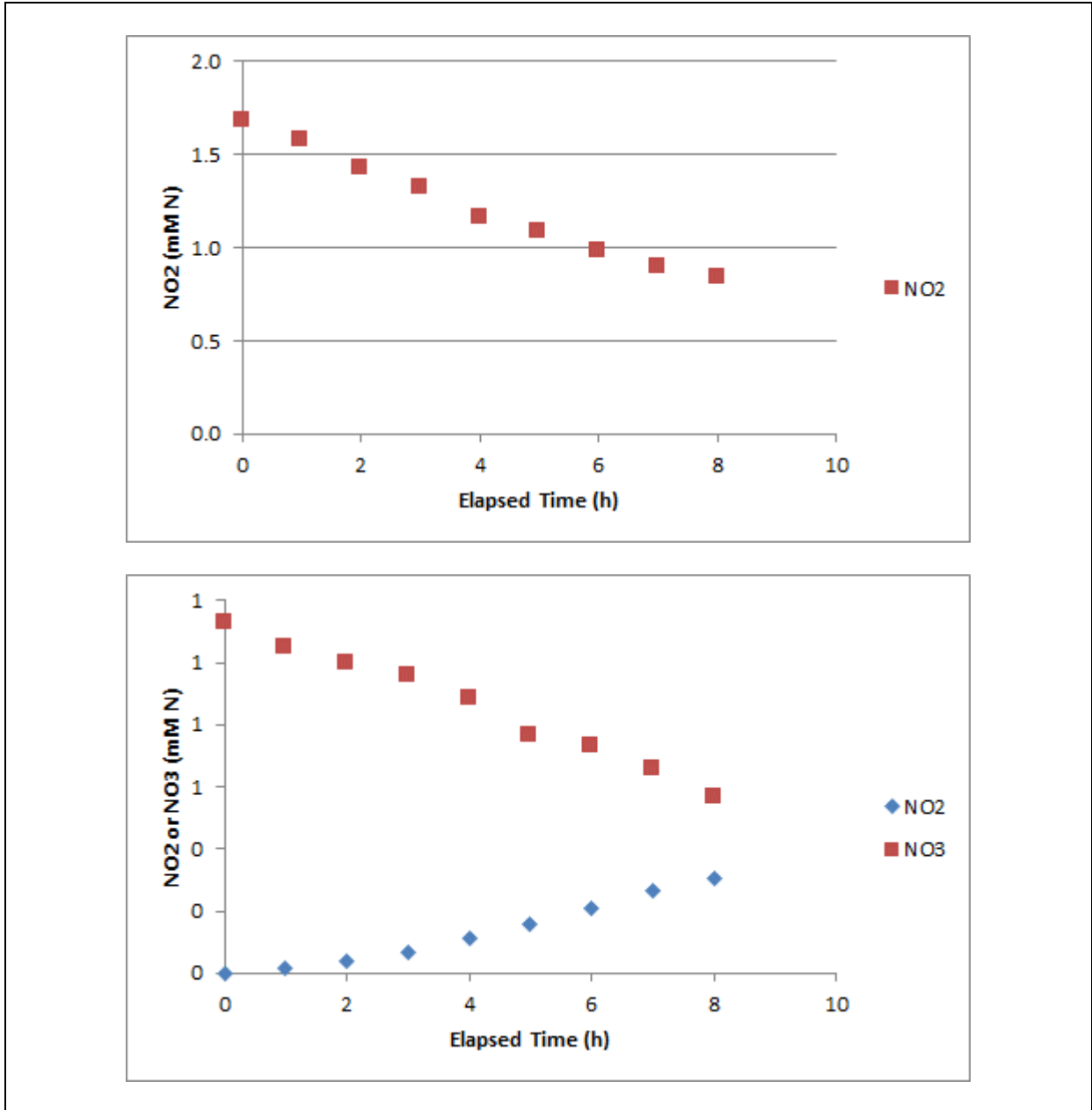


Figure 2.4-5. Cathodic degradation of nitrite (top) and nitrate (bottom) in the IrO₂ electrode system

2.4.8 Cathodic degradation of NC fines

2.4.8.1 Methods.

Degradation of NC Fines was performed using the IrO₂ system by packing a small amount of NC (1.5 g dry wt) into the in-line strainer and placing the strainer in the cathodic loop. The degradation was performed at a constant voltage of 4 V, with an initial catholyte volume of 380 ml of 1000 mg/L sulfate and an initial anolyte volume of 3800 ml of 5000 mg/L sulfate. Samples were collected periodically over several days and analyzed for pH, anions, TOC, and DPD; samples were also titrated to determine H⁺ and OH⁻ molarity in the anolyte and catholyte, respectively. After several days the power was switched off while the pump remained on.

Another experiment was performed to determine how NC degraded in a flow through configuration in the presence of base equivalent to what was generated in the electrochemical cell. This was done to allow comparison to the observed NC degradation using electrochemically generated hydroxide. A solution was prepared containing approximately 1000 mg/L sulfate and 0.3 N NaOH equivalent, which was roughly equivalent to the catholyte hydroxide molarity during the electrochemical NC degradation testing. The electrochemical cell was removed from the loop during this experiment, but the flow rate remained the same. Once flow was started, samples were removed periodically to measure the concentrations of released anions (nitrate and nitrite), as well as to monitor pH, hydroxide concentration, TOC and COD.

2.4.8.2 Results and Discussion.

Degradation of NC Fines was performed by packing a small amount of NC (1.5 g dry wt) into the in-line strainer and placing the strainer in the cathodic loop. The electrochemical experiment was performed at a constant voltage of 4 V, with an initial catholyte volume of 380 ml of 1000 mg/L sulfate and an initial anolyte volume of 3800 ml of 5000 mg/L sulfate. Samples were collected periodically over several days and analyzed for pH, anions, TOC, and DPD; samples were also titrated to determine H⁺ and OH⁻ molarity in the anolyte and catholyte, respectively. After several days the power was switched off while the pump remained on.

During the first test, the pH measured by the probe in the cathodic loop reached 12 after 3.5 days, with a hydroxide concentration of 0.29 N. Only 54% of the initial mass of NC remained in the strainer at the end of the experiment, and the residual mass had a nitrogen content (12.1 %N), similar to the starting material (12.5 %N). The measured dissolved nitrite plus nitrate (as N) vs time is shown in **Figure 2.4-6** (top), and represents 24% denitration of the NC. However, nitrogen species were also being degraded as they were being produced. Therefore, the nitrogen data was corrected based on results presented in section 2.1.5 above. **Figure 2.4-6** (bottom) presents the corrected nitrogen data, and represents 54% degradation of the initial NC, which is comparable to degradation based on the observed NC mass loss from the strainer (46%). Residual total carbon (TC) and chemical oxygen demand (COD) in the solution at the end of the test only accounted for

5 to 10% of the initial NC mass (on a carbon basis), indicating that carbon released from the NC during hydrolysis was further broken down or otherwise undetectable.

During the second test, the pH measured by probe in the cathodic loop again reached 12 after 4.5 days, but had a slightly higher hydroxide concentration (0.33 N) than seen during the first run. Only 33% of the initial mass of NC remained in the strainer at the end of the experiment, with a nitrogen content of 12.0 %N (again, not significantly different from the starting material, 12.5 %N). The measured dissolved nitrite plus nitrate (as N) and the corrected nitrogen released are shown in **Figure 2.4-7**, and represent 17% and 76% denitration, respectively. The 76% NC degradation based on the corrected released nitrogen was comparable to the degradation based on residual NC mass in the strainer (e.g., 67%). As in the first test, residual TC and COD for less than 10% of the initial NC mass (carbon basis), indicating that carbon released from the NC during hydrolysis was again further broken down or otherwise undetectable.

During the test in which alkaline hydrolysis was performed under flow conditions with a 0.3 N NaOH initial hydroxide concentration, nitrogen release (sum of NO₂ and NO₃) as a function of time clearly demonstrated NC degradation (**Figure 2.4-8**). However, the rate of NC degradation appeared to slow over time, likely as the result of the decreasing hydroxide concentration in the circulating solution (**Figure 2.4-9**). Approximately 53% of the NC mass was degraded over the course of the experiment. based on released nitrogen. This is close to the 49% degradation based on the TC measured in the solution at the end of the experiment. This TC measurement is significantly higher than that observed during the first two tests with the electrochemical cell powered up, and indicates that NC hydrolysis using just hydroxide results in the formation residual carbonaceous breakdown products that are not further broken down in the alkaline solution.

A comparison of degradation of NC by electrochemically generated hydroxide and hydroxide from NaOH (this current experiment) is shown in **Figure 2.4-10**. The degradation rate in the electrochemical system started slowly but then increased. This was likely due to lower initial, but then increasing, hydroxide concentrations (**Figure 2.4-11**). In contrast, the degradation rate in the NaOH only experiment started relatively faster than the electrochemical experiments, but then slowed markedly over time. As stated above, this likely reflects the higher initial hydroxide concentration, followed by the slow decrease in hydroxide concentrations. The approximate energy demand for a 50% decrease in NC mass in test 2 was 10 W-h L⁻¹.

The data from **Figures 2.4-10** and **2.4-11** were more closely examined to compare the efficiency of NC denitration as a function of hydroxide concentration during bulk hydrolysis and the electrochemical process. As can be seen in **Figure 2.4-12**, the electrochemical process appears to be 50 to 60% more efficient at any given hydroxide concentration, although the exact mechanism is not known at this time. It may be the result of oxidant reactions, although the bulk catholyte DPD values were relatively low during these experiments. Another possibility is that as the

process progresses, the NC begins to depolymerize, allowing some NC from the strainer to migrate to the electrochemical cell. The NC would then be exposed to significantly higher local hydroxide (or oxidant) concentrations near the cathode, or the NC could possibly undergo direct denitration upon contact with the cathode surface. Additional investigation is needed to determine which mechanisms are responsible for the higher denitration rates during the electrochemical process.

Overall, these series of experiments indicate the potential advantage of electrochemical degradation of NC fines compared to traditional alkaline hydrolysis, including:

- 1) The improved safety of in situ hydroxide generation compared to handling caustics.
- 2) The ongoing generation of hydroxide to drive the NC degradation process.
- 3) The concurrent degradation of both the parent NC by the circulating hydroxide and the nitrite/nitrate breakdown products within the electrochemical cell.
- 4) The continued, albeit slower, denitration of NC by the elevated hydroxide even after the power is turned off.
- 5) The potential to auto-neutralize the final solution by mixing the anolyte and the catholyte at the end of the process.

2.4.8.3 Preliminary process and cost effectiveness comparison.

The results obtained are not assumed to be under the optimized conditions. However, based on these results, and information available from the literature, a preliminary cost comparison with the standard (bulk) NC alkaline hydrolysis process was performed.

The stoichiometry indicates that 1 kg of KOH is needed to completely hydrolyze 1 kg of NC. However, the literature describing larger scale processing of NC fines indicates that the ratio to achieve complete hydrolysis of the NC is closer to 2 kg KOH per kg NC (36).

Using this as a starting point, the costs to degrade 1 kg of NC were calculated based on the standard bulk process and based on the generation of the equivalent OH^- via the electrochemical process. The other costs for the actual processing of the NC (e.g., power for mixing, acid for neutralization, etc.) are assumed to be the same regardless of the source of the hydroxide, and the capital costs for the electrochemical cell parts are not included. The results presented in **Table 2.4-1** demonstrate that on the basis of hydroxide generation, the electrochemical process is quite comparable to use of bulk KOH. *However, it should be noted that the cost listed in the electrochemical treatment column represents generating the total alkali equivalent based on bulk NC hydrolysis. The cost does not reflect the expected greater efficiency of the electrochemical process based on the data presented in Figure 2.4-12, which would reduce the total cost by 50 to 60% (e.g., ~\$1.25/kg). Additionally, further efficiency increases would be expected as the electrochemical process is optimized, leading to even lower treatment costs.*

As a ground-truthing exercise, the power requirement for generating hydroxide in our non-optimized small test system was also comparable to what has been reported for industrial scale

hydroxide production using the chlor-alkali process (~6 kW-h; http://www.inference.org.uk/sustainable/LCA/elcd/external_docs/naoh_31116f0a-fabd-11da-974d-0800200c9a66.pdf).

Additional work would be required to complete a more accurate cost comparison between the standard bulk NC hydrolysis method and an electrochemical approach. Beyond increasing safety and generating the required hydroxide at a comparable cost, the data generated thus far also indicate that the electrochemical approach also appears to be more efficient than bulk hydrolysis, although the mechanisms are not yet known.

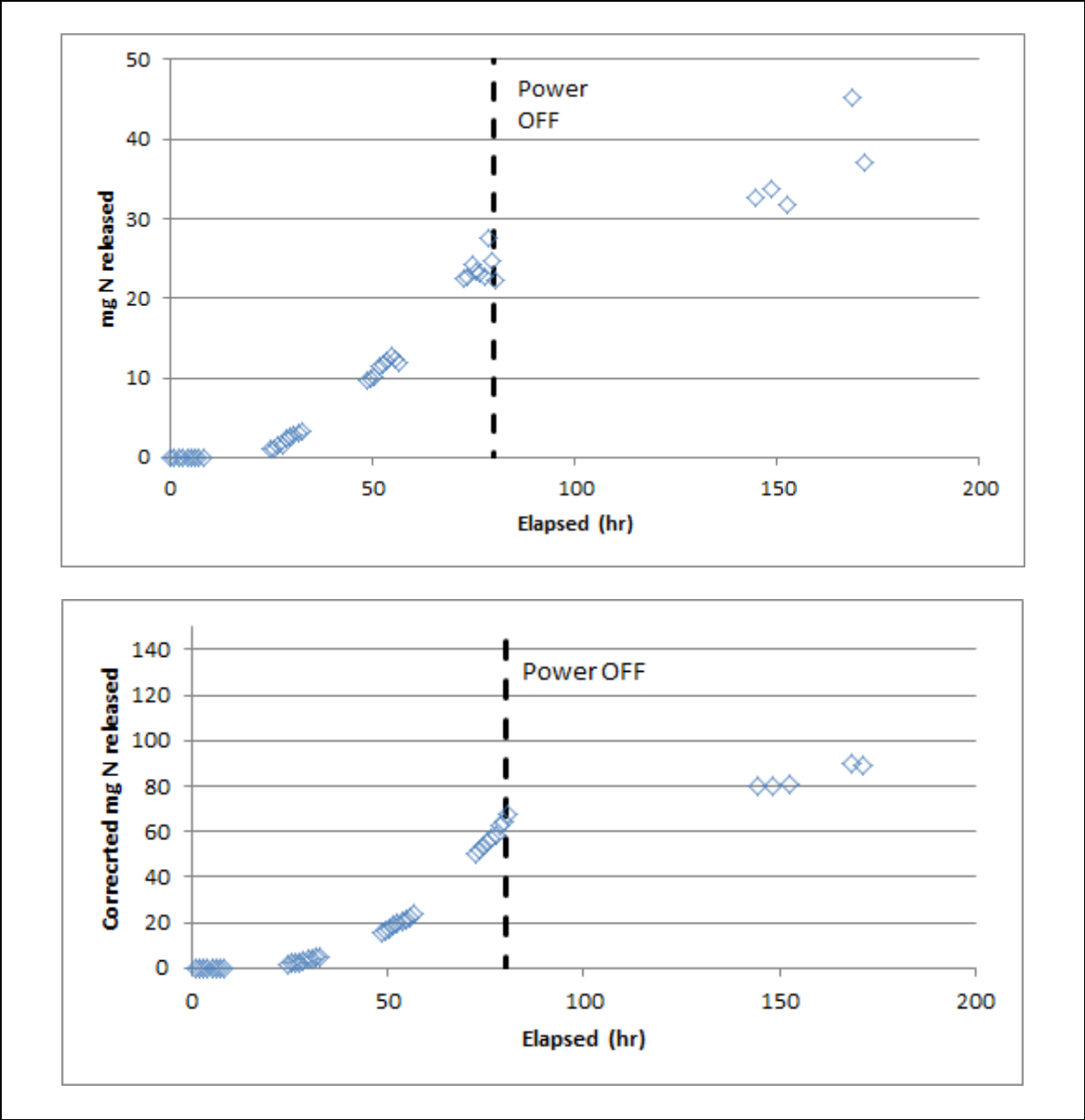


Figure 2.4-6. Denitration of NC during the first test based on measured mass of nitrogen released (nitrite plus nitrate) (top) and corrected mass of nitrogen released (bottom) the IrO₂ electrode system.

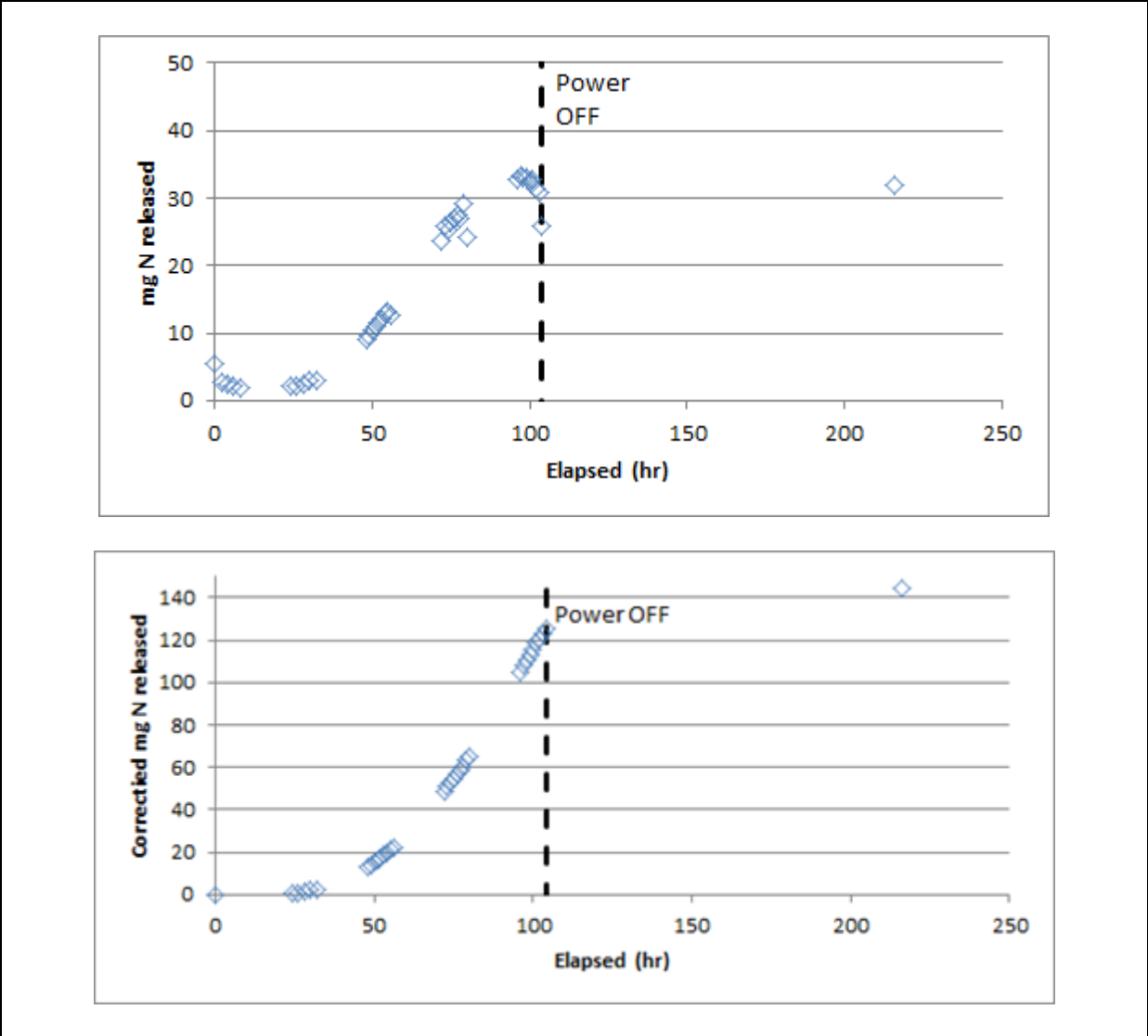


Figure 2.4-7. Denitration of NC during the second test based on measured nitrite plus nitrate released (top) and corrected mass of nitrogen released (bottom) the IrO₂ electrode system.

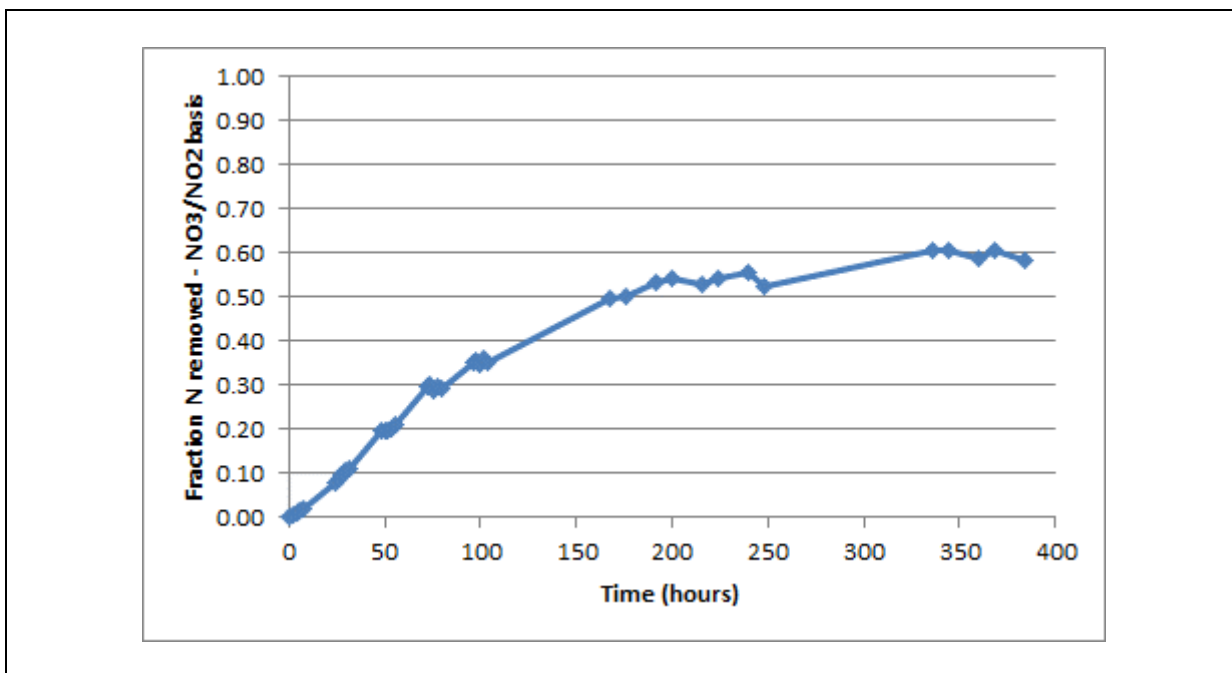


Figure 2.4-8. Production of nitrite and nitrate during alkaline hydrolysis of NC in a flow through configuration with an initial hydroxide concentration of 0.3 N.

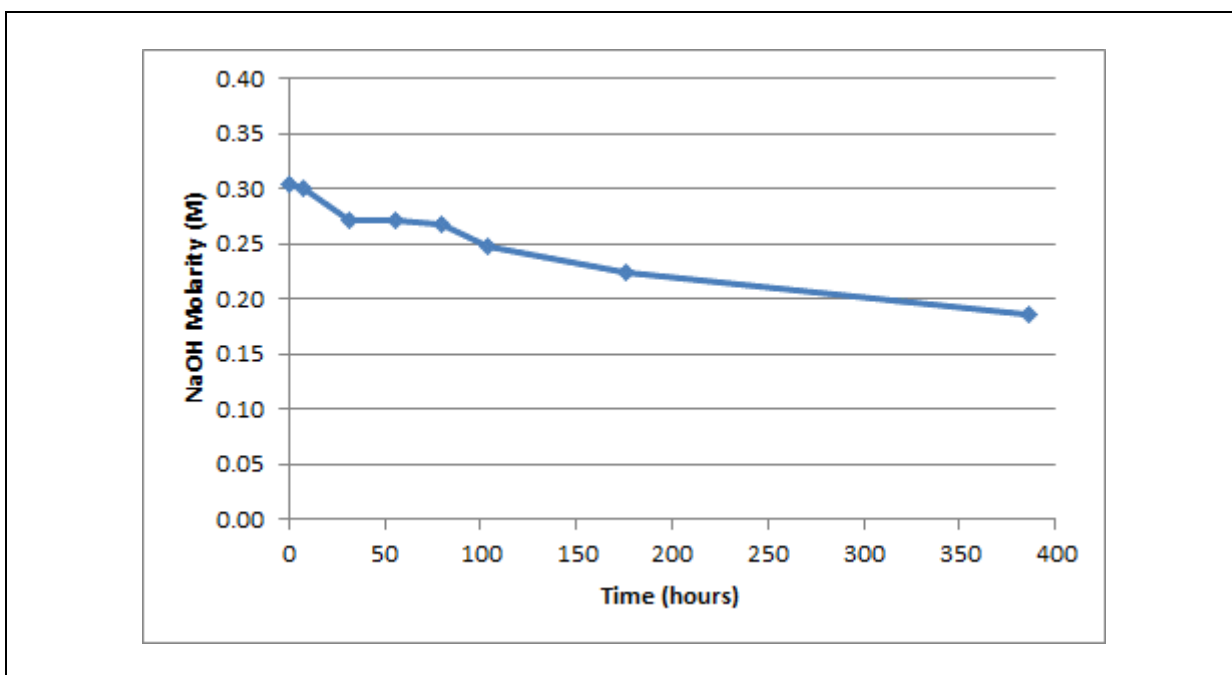


Figure 2.4-9. Changes in hydroxide concentration over time during alkaline hydrolysis of NC in a flow through configuration with an initial hydroxide concentration of 0.3 N.

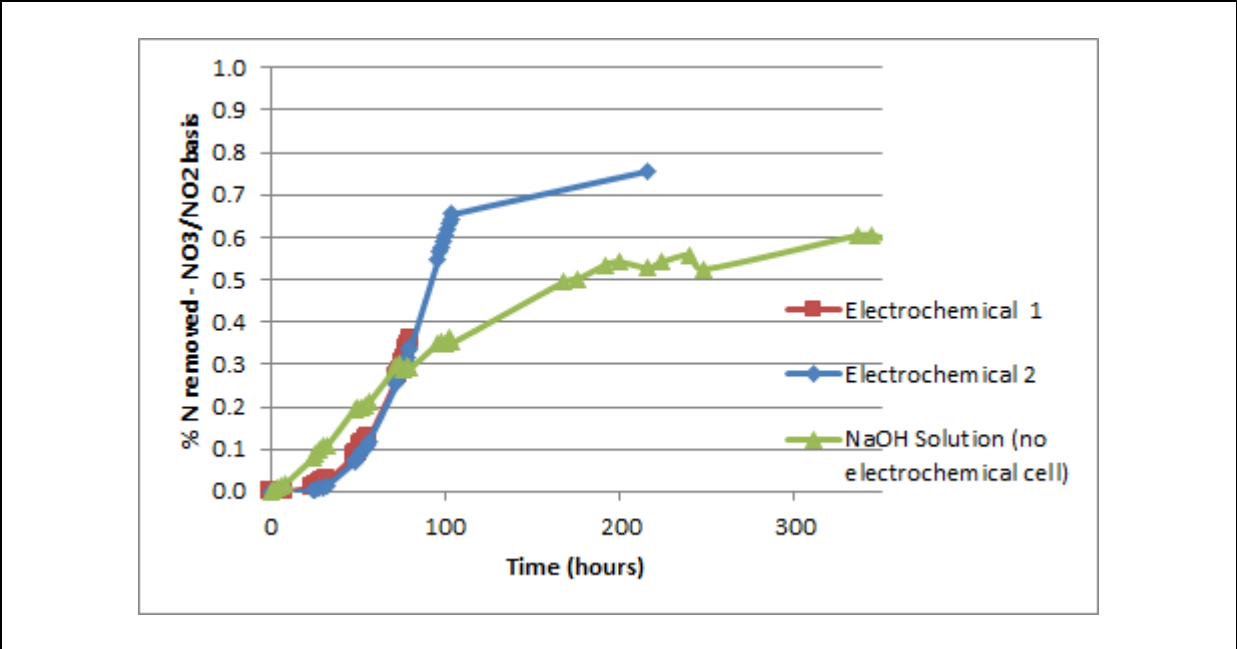


Figure 2.4-10. Comparison of nitrate and nitrite production during alkaline hydrolysis of NC with 0.3 N hydroxide (added as NaOH) and electrochemically generated hydroxide in a flow through configuration.

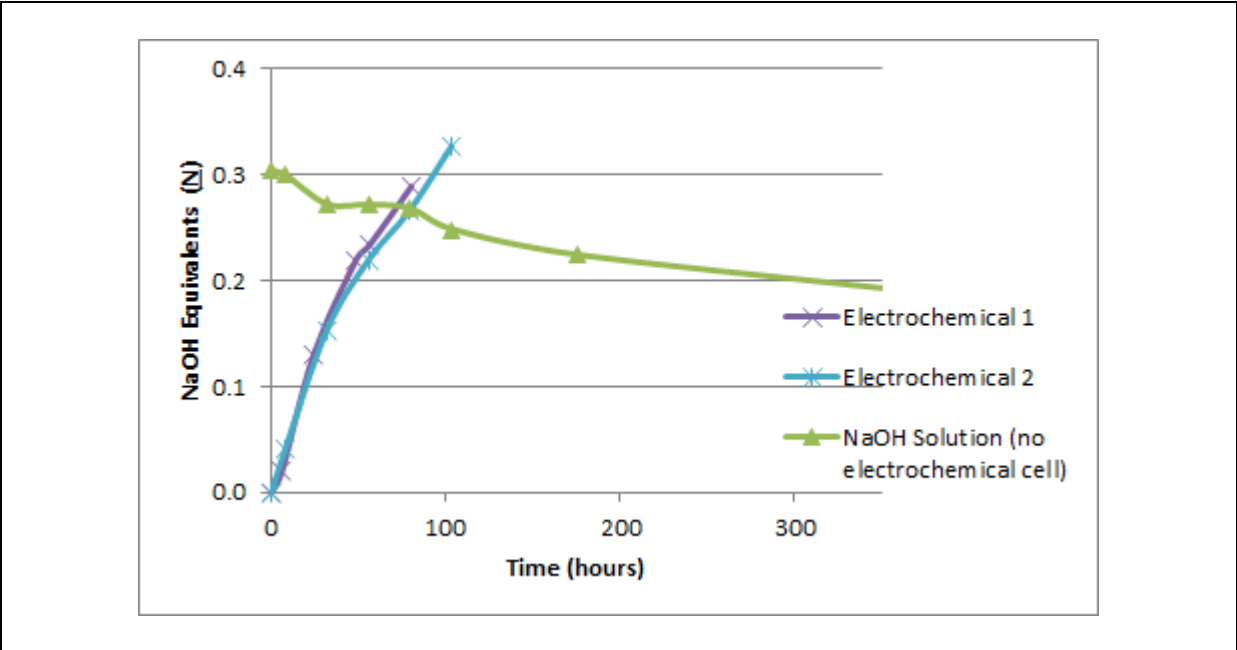


Figure 2.4-11. Comparison of hydroxide molarity during alkaline hydrolysis with 0.3 N hydroxide (added as NaOH) and electrochemically generated hydroxide in a flow through configuration.

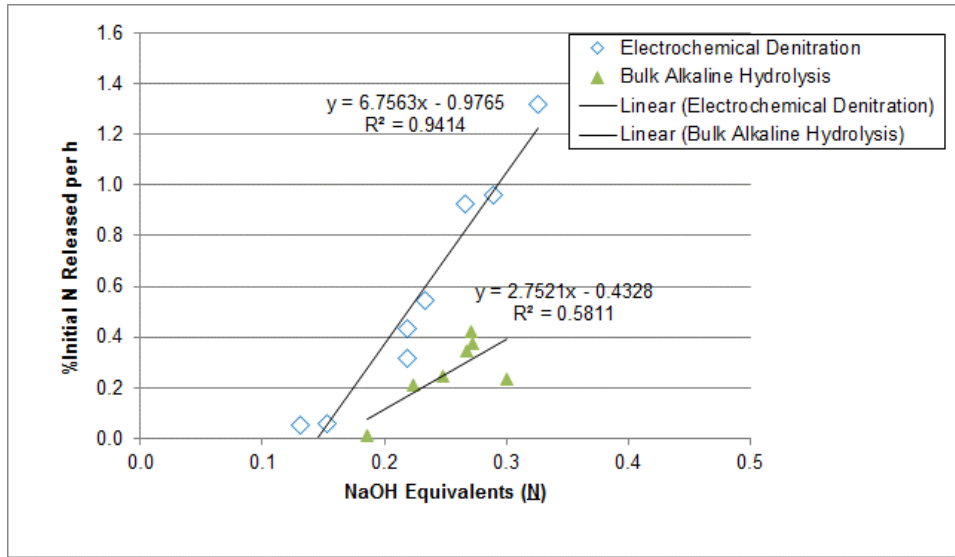


Figure 2.4-12. Comparison of the NC denitration rate (expressed as percent of the initial nitrogen in the NC released) during alkaline hydrolysis with 0.3 N hydroxide (added as NaOH) and electrochemically generated hydroxide in a flow through configuration.

Materials and Cost Elements		Bulk Alkaline Hydrolysis	Electrochemical Hydrolysis
Mass NC	kg	1	1
Alkali requirement (KOH) per 1 kg NC	kg	2	2
Alkali cost (solid KOH)	\$/kg	1.16 ^a	
Alkali cost to meet alkali requirement	\$	2.32	
Power to generate 0.4 molar OH	kW-h/L		0.16
Power to generate 1 molar OH	kW-h/L		0.40
1 molar KOH =	0.056 kg KOH		
Power to generate 1 kg KOH	kW-h/L		7.12
Power to generate alkali requirement	kW-h/L		14.23
Volume of reactor	L		2
Electricity rate	\$/kW-h		0.09
Electricity cost to generate required kg KOH	\$		2.56
TOTAL COST		2.32	2.56 ^b

^a Average of medium and very large bulk KOH commodity prices found on the following websites:

<https://www.alibaba.com/showroom/potassium-hydroxide-price.html>

<https://www.utahbiodieselsupply.com/biodieselchemicals.php>

<http://www.infomine.com/investment/metal-prices/potash/all/>

^b Cost represents generating the total alkali equivalent based on bulk NC hydrolysis. Cost does not reflect the expected greater efficiency of the electrochemical process based on the data presented in Figure 2.4-12, which would reduce the total cost by 50 to 60% (e.g., ~\$1.25/kg).

Table 2.4-1. Comparison of cost of bulk NC hydrolysis and electrochemical NC degradation based on alkali requirement.

2.5 Task 5 – Longer-term degradation of RDX in divided cell configuration

2.5.1 Goal and Introduction

In light of the overall project goal

To evaluate which electrochemical designs would be effective for explosive and propellant treatment with respect to specific anodes and cell configurations.

The focus of this task was to evaluate any changes in the cathodic degradation of RDX in the divided cell configuration over a longer-time period, noting any changes in operational parameters or degradation kinetics.

2.5.2 RDX degradation at constant voltage

2.4.2.1 Methods.

Prior to starting experiments to assess electrode longevity and performance, two tests were performed to examine cathodic RDX degradation with the IrO₂ anode/SS cathode in the divided configuration under constant voltage, as opposed to constant current. Experiments were run at a constant voltage of 4 V, which was previously determined to be in the correct range to avoid excessive water splitting reactions (e.g., wasted energy) during the degradation process (see section 2.4.5). The electrolyte was 1000 mg/L sulfate and the flow rate was 0.1 L/min.

2.5.2.2 Results.

In duplicate experiments, RDX was degraded at an average rate of 0.18 h⁻¹, and the major transformation products were nitrite (with trace nitrate) and NDAB (**Figure 2.5-1**). For comparison, **Table 2.5-1** presents these results along with those from the undivided and divided cell configuration run at a constant current of 0.5 A. The RDX degradation rate coefficient under constant voltage was approximately 50% of that under constant current (0.18 vs. 0.36 /h). However, the CE under constant voltage was over 13-fold higher than under constant current (1.12 vs. 0.08%). These results suggest that operation at the lower applied voltages results in a much greater RDX treatment efficiency, likely due to the absence of substantial water electrolysis.

Consistent with the improved current efficiency, the energy for 50% removal in the divided cell is 3.2 W-h L⁻¹ (only cathodic RDX transformation was observed). This is approximately an order of magnitude less than that observed at elevated currents. In addition, the relationship between the applied current and the observed RDX transformation rate constant suggest that the limiting current density on the cathode is well below 50 mA/cm². Thus, as previously demonstrated, operating at such elevated current densities results in poor CE and energy efficiency.

The final catholyte pH was approximately the same in both tests (11.5 S.U.), while the maximum catholyte DPD was about 50% lower under constant voltage than under constant current. Additionally, the constant voltage test exhibited higher residual nitrite+nitrate compared to the constant current test (0.05 vs. 0.18 expressed as fraction of initial mM RDX nitrogen).

The nitrite+nitrate and NDAB detected represent approximately 25 to 30% of the RDX on a nitrogen basis, and appeared to be stable in the cathodic loop. To assess further breakdown of these products, the residual test solution from the duplicate experiments was combined and placed in the cathode loop for several days. The results in **Figure 2.5-2** did confirm additional degradation nitrite and nitrate at a constant voltage of 4 V, albeit with lower rate coefficients of 0.02, and 0.04 /h, respectively, compared to 0.9 and 0.08 /h during previous experiments at a constant current of 0.5 A. NDAB was degraded with a rate coefficient of 0.05 /h.

The remainder of the RDX (as nitrogen) was likely present as compounds that are not detectable by our methods, or escaped from the system as gaseous products (e.g., N_2O).

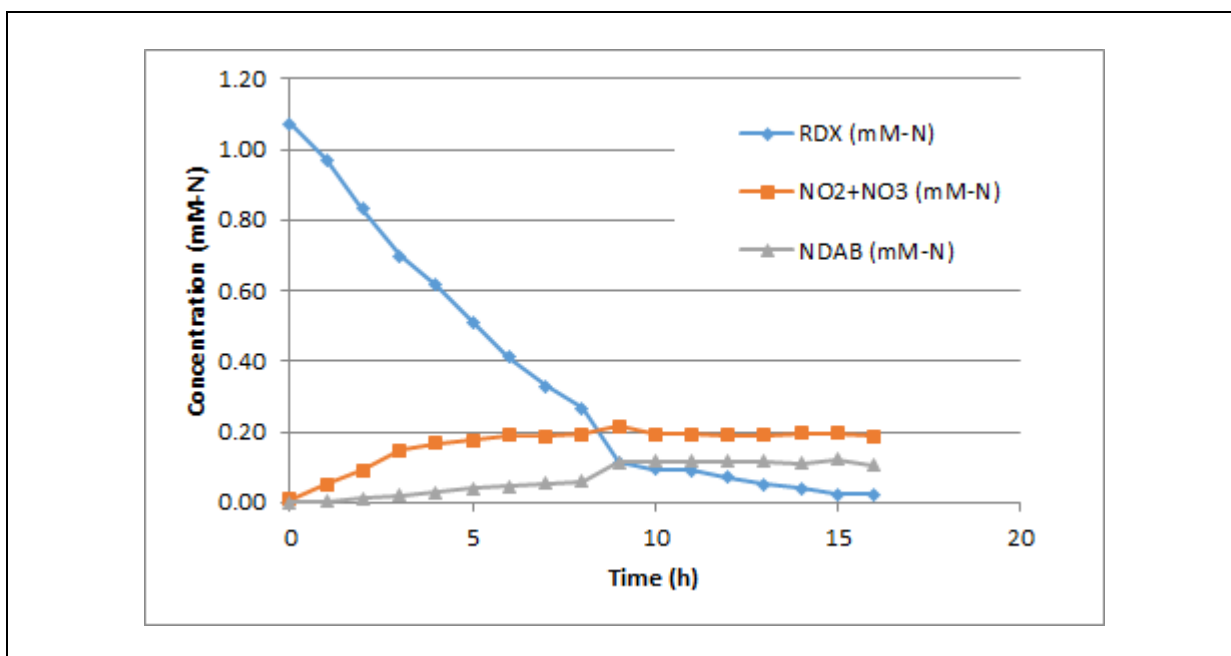


Figure 2.5-1. Cathodic transformation of RDX in the divided cell configuration with the IrO_2 anode and SS cathode at a constant voltage of 4 V.

Anode	Cathode	Configuration	RDX in Catholyte or Anolyte	Flow Rate (L/min)	Na ₂ SO ₄ Electrolyte (mg/L)	Maximum Voltage (V)	Maximum Current (A)	Final pH (S.U.)	Maximum DPD Oxidant (absorbance)	RDX Degradation Rate			Recovery of NO ₂ +NO ₃ Relative to Initial RDX (mM-N)	
										-k (1/h)	±SE	r ²	RDX (mM-N)	CE (%)
IrO ₂	SS	Undivided	N/A	0.10	1000	10	0.50	8.9	0.03	0.22	0.02	1.00	0.05	0.06
IrO ₂	SS	Divided	Catholyte	0.10	1000	10	0.50	11.4	0.04	0.36	0.06	0.99	0.05	0.08
			Anolyte	0.10	1000	10	0.50	2.3	0.19	0.00	0.00	0.67	0.00	0.00
IrO ₂	SS	Divided	Catholyte	0.10	1000	4	0.04	11.5	0.02	0.18	0.01	0.99	0.18	1.77

Table 2.5-1. RDX degradation rate confidents and other parameters for experiments with the IrO₂ anode and SS cathode at a constant voltage or constant current.

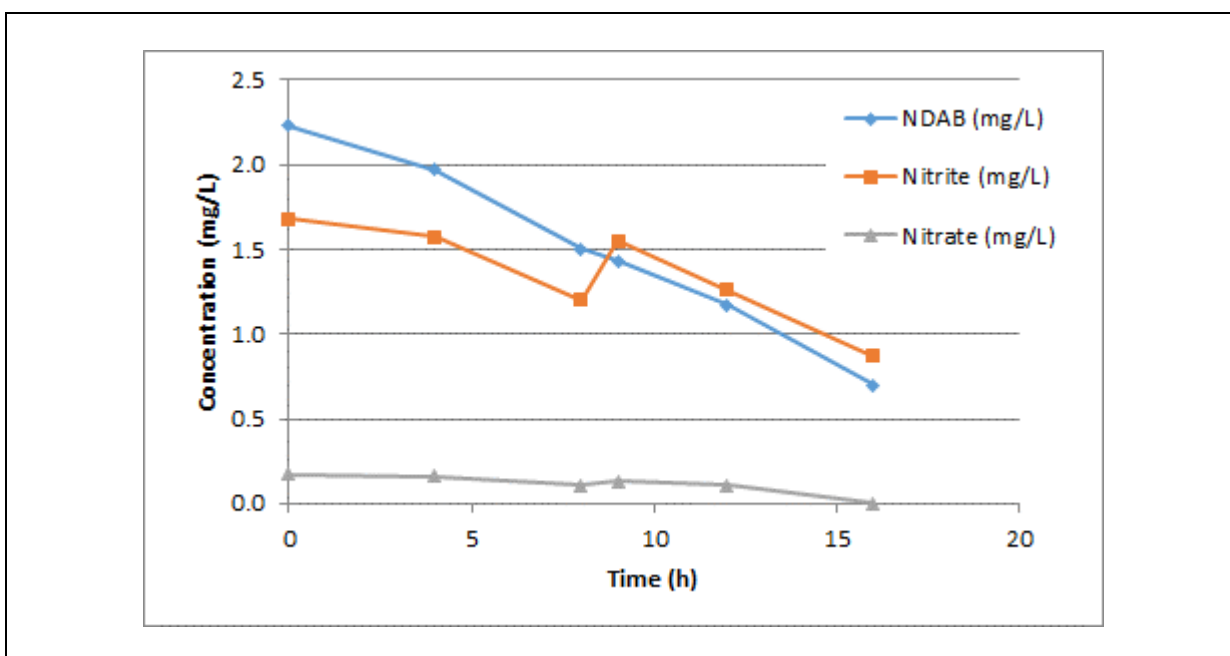


Figure 2.5-2. Degradation of NDAB, nitrite, and nitrate in the divided cell configuration with the IrO₂ anode and SS cathode at a constant voltage of 4 V.

2.5.3 Multirun testing of RDX degradation

2.4.3.1 Methods.

Longer term testing was performed over several weeks, using the following test parameters:

- Configuration: Divided flow cell
- RDX: Approximately 30 to 40 mg/L
- Anode: IrO₂
- Cathode: SS
- Membrane: DuPont Nafion® 117 (cation exchange membrane, 0.17 mm thickness)
- Gap: 8 mm (distance between anode and cathode)
- Electrode Area: 10 cm²

-Initial Volume: 0.35 L
-Flow rate: 0.1 L/min (recirculation)
-Voltage: Constant voltage @ 4 V
-Electrolyte: 1000 mg/L SO₄⁻

Each test lasted eight hours. The voltage and current were monitored and recorded. Samples of the catholyte were collected at 0, 3, 5 and 8 h for analysis of RDX, RDX breakdown products, and anions. Sample were diluted 1:1 with 1 M phosphate buffer to prevent RDX breakdown and NDAB formation in the interval between sample collection and analysis.

Samples were collected from both the anolyte and the catholyte at the end of each test for pH, DPD, and titration, and from the catholyte for TOC and COD analysis. At the end of each test, the system was flushed with distilled water. At the end of every fifth test, the norprene pump tubing was replaced. At the end of test six and every fifth test thereafter, the electrochemical cell was operated in reverse polarity mode for twenty minutes to remove any precipitates and thus prevent fouling of the electrodes (especially the cathode).

2.5.3.2 Results.

The RDX degradation rate coefficient ($-k$, 1/h) for each test is shown in **Figure 2.5-3**. The rate coefficient cycled overtime, averaging $0.18 \pm 0.02/h$ ($n=24$). The cyclic nature roughly parallels the timing of both the pump head tubing changes and the defouling activities. These results indicate minimal decrease in RDX degradation efficiency over time, and relatively robust system longevity.

The concentrations of nitrite and NDAB, and the nitrogen mass balance, at the end of each test is shown in **Figure 2.5-4**. The amount of NDAB present at the end of each test slowly drifted upward from 0.05 to 0.1 mM, while residual nitrite rose from 0.07 mM to approximately 0.17 mM, with some variability from test to test. This may indicate some decrease in and NDAB nitrite degradation efficiency at the SS cathode, thereby leading to more net accumulation of nitrite in each test. This increase in residual NDAB and nitrite also lead to slow doubling in the nitrogen mass balance values for the latter tests (from 12% to 25%).

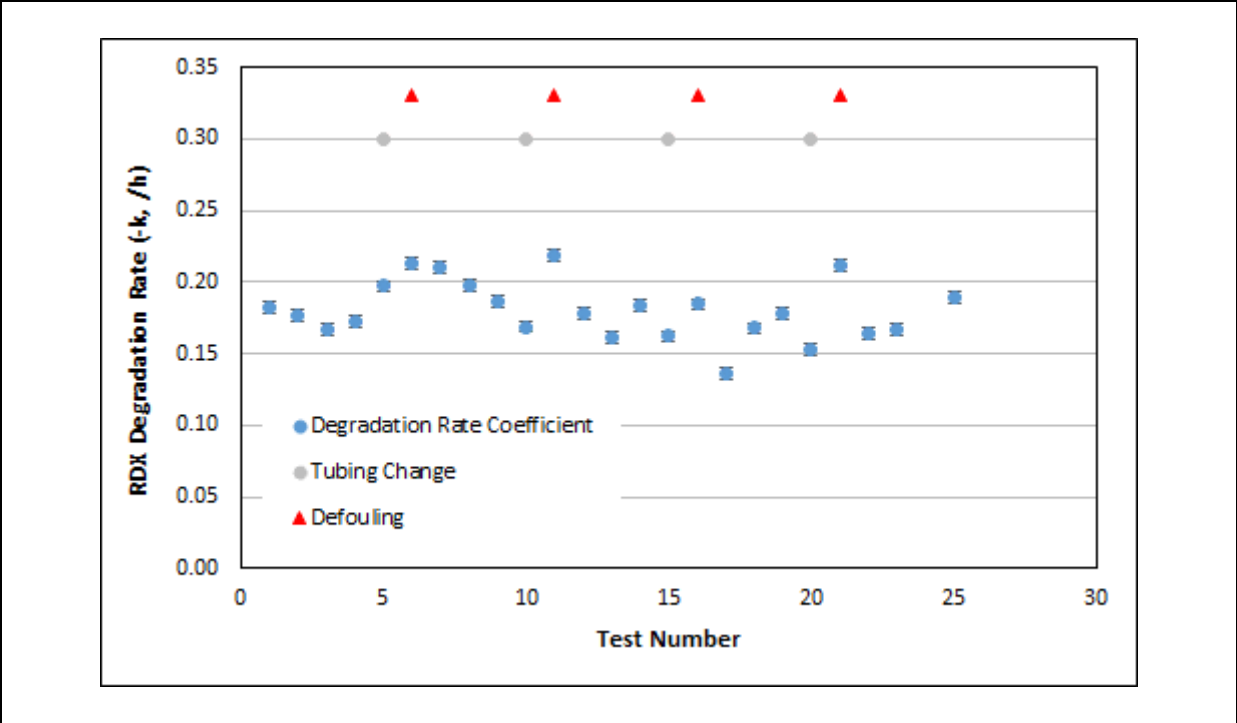


Figure 2.5-3. RDX degradation rate coefficient for each test during the longer term evaluation.

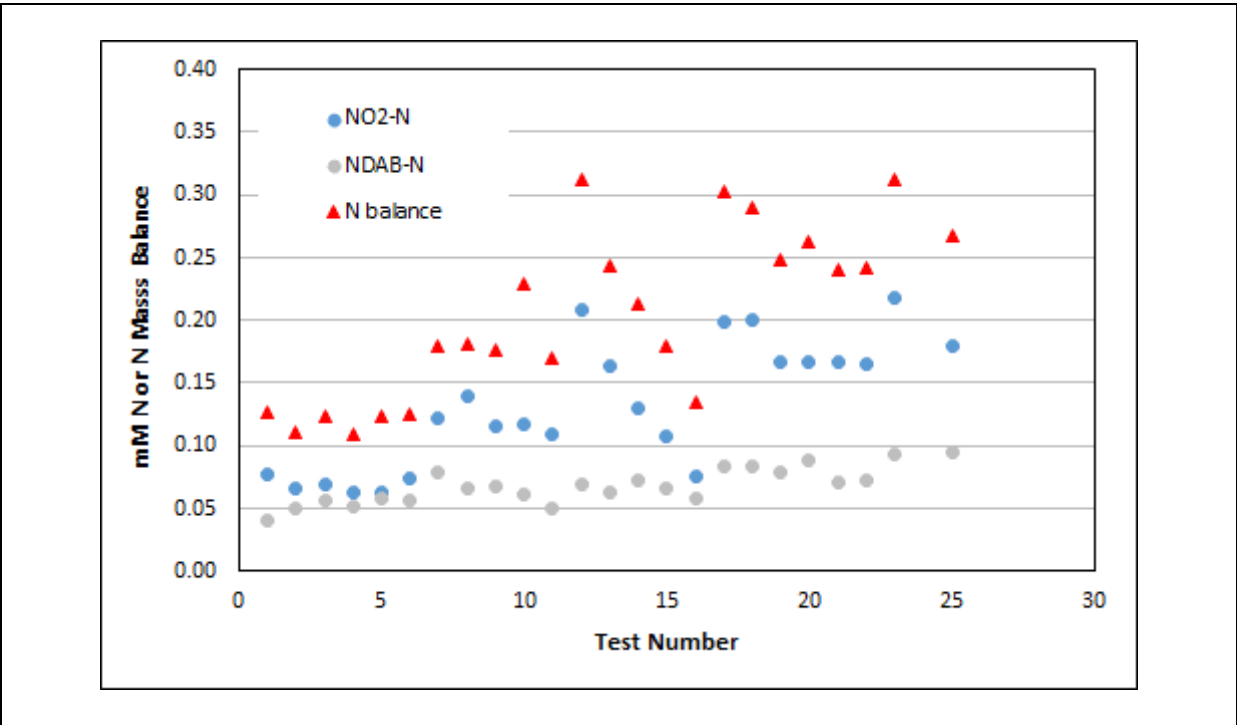


Figure 2.5-4. Concentration of nitrite and NDAB, and the nitrogen mass balance, at the end of each test during the longer term evaluation.

3.0 CONCLUSIONS AND IMPLICATIONS FOR FUTURE RESEARCH

3.1 Key results

This project produced solid proof-of-concept data that supports further investigation of electrochemical demilitarization of explosives and energetics. This project used a small-scale electrochemical system and single representative compounds (RDX and NC) to minimize the analytical complexity and allow multiple variables to be clearly compared.

For dissolved RDX (as a representative explosive), the key results of this project were as follows:

- In an undivided cell configuration with constant current:
 - Electrochemical degradation of dissolved RDX was demonstrated with both BDD and MMO anodes coupled to SS cathodes.
 - Degradation rates were slightly higher with the BDD anode than with the MMO anodes, but more net RDX breakdown products (nitrite and nitrate) were produced with the BDD anode.
 - Modest changes in electrolyte concentration (10-fold) and flow rate (2-fold) only resulted in 10 to 20% changes in the RDX degradation rate coefficient.

- In a divided cell configuration with constant current:
 - Both anodic and cathodic degradation of dissolved RDX was demonstrated with BDD anode coupled to a SS cathode. This indicates the potential for sequential cathodic/anodic treatment with increased degradation efficiency (e.g., higher mass degraded per unit of energy expended).
 - Robust RDX degradation was only observed cathodically with an IrO₂ anode coupled to a SS cathode.
 - Cathodic degradation rates were higher in the divided configuration compared to the undivided configuration, which was attributed to the more alkaline conditions in the catholyte in the divided cell configuration.

- In a divided cell configuration with constant voltage:
 - Cathodic RDX degradation rates with an IrO₂ anode coupled to a SS cathode were relatively stable over repeated tests, indicating good longevity of the electrodes.

For NC, this project performed the first known demonstration of alkaline hydrolysis of solid nitrocellulose via electrochemically generated hydroxide using an IrO₂ anode coupled to a SS cathode operated in divided cell configuration with constant voltage. The nitrite, nitrate, and carbonaceous breakdown products generated were partially degraded as the NC was hydrolyzed. The preliminary data indicated that the electrochemical process was 50-60% more efficient than bulk alkaline hydrolysis based on the rate of NC denitration.

3.2 Suggested follow-on work

Based on the research conducted during this project, the steps recommended to move this electrochemical demilitarization technology forward are listed below. Some of the activities are need to more fully characterize the degradation process, while others will serve to move the technology forward and lay the foundation for pilot-scale testing and implementation.

- Perform experiments to specifically address outstanding mechanistic questions:
 - Employ additional analytical techniques to determine the final end products of RDX and NC degradation.
 - Close the carbon and nitrogen mass balances.
 - Perform a more detailed evaluation of sequential cathodic/anodic treatment of RDX.
 - Better define the contributions of alkaline hydrolysis, oxidants, and electrode surface reactions in RDX and NC breakdown.
 - Evaluate treatment of insensitive high explosives.
- Evaluate electrochemical treatment of mixtures of explosives (e.g., typical of LAPP wastestreams, including insensitive high explosives).
- More fully examine the degradation of solid energetics (e.g., NC fines, M6 propellant pellets) using a larger bench-scale system with specific attention to identifying and minimize potential mass-transfer limited processes.
- Design and test a mid-sized system for electrochemical destruction of nitrocellulose fines to integrate with existing Picatinny Arsenal/ARDEC demilitarization activities.

4.0 REFERENCES CITED

1. **Atkins, P. W.** 1997. *Physical Chemistry*. 6th Edition. W.H. Freeman and Company, New York.
2. **Azizi, O., D. Hubler, G. Schrader, J. Farrell, and B. P. Chaplin.** 2011. Mechanism of perchlorate formation on boron-doped diamond film anodes. *Environmental Science & Technology* **45(24)**: 10582-10590.
3. **Balakrishnan, V. K., A. Halasz, and J. Hawari.** 2003. Alkaline hydrolysis of the cyclic nitramine explosives RDX, HMX, and CL-20: New insights into degradation pathways obtained by the observation of novel intermediates. *Environmental Science & Technology* **37(9)**: 1838-1843.
4. **Bonin, P. M. L., D. Bejan, L. Schutt, J. Hawari, and N. J. Bunce.** 2004. Electrochemical reduction of hexahydro-1,3,5-trinitro-1,3,5-triazine in aqueous solutions. *Environmental Science & Technology* **38(5)**: 1595-1599.
5. **Cabeza, A., A. M. Urtiaga, and I. Ortiz.** 2007. Electrochemical treatment of landfill leachates using a boron-doped diamond anode. *Industrial & Engineering Chemistry Research* **46(5)**: 1439-1446.
6. **Chen, Y., L. Hong, W. Han, L. Wang, X. Sun, and J. Li.** 2011. Treatment of high explosive production wastewater containing RDX by combined electrocatalytic reaction and anoxic-oxic biodegradation. *Chemical Engineering Journal* **168(3)**: 1256-1262.
7. **Chen, Y., L. Hong, W. Shi, W. Q. Han, and L. J. Wang.** 2012. Electrochemical degradation of RDX in aqueous solution at constructed Sb-doped SnO₂ anode. *Advanced Materials Research* **396-398**: 1803-1806.
8. **Comninellis, C., A. Kapalka, S. Malato, S. A. Parsons, I. Poulios, and D. Mantzavinos.** 2008. Advanced oxidation processes for water treatment: advances and trends for R&D. *Journal of Chemical Technology & Biotechnology* **83(6)**: 769-776.
9. **Davis, J. L., M. C. Brooks, S. L. Larson, C. C. Nestler, and D. R. Felt.** 2006. Lime treatment of explosives-contaminated soil from munitions plants and firing ranges. *Soil & Sediment Contamination* **15(6)**: 565-580.
10. **De, D., E. E. Kalu, P. P. Tarjan, and J. D. Englehardt.** 2004. Kinetic studies of the electrochemical treatment of nitrate and nitrite ions on iridium-modified carbon fiber electrodes. *Chemical Engineering & Technology* **27(1)**: 56-64.
11. **Deligiorgis, A., N. P. Xekoukoulotakis, E. Diamadopoulos, and D. Mantzavinos.** 2008. Electrochemical oxidation of table olive processing wastewater over boron-doped diamond electrodes: Treatment optimization by factorial design. *Water Research* **42(4-5)**: 1229-1237.
12. **El-Ghenmy, A., F. Centellas, J. A. Garrido, R. M. Rodríguez, I. Sirés, P. L. Cabot, and E. Brillas.** 2014. Decolorization and mineralization of Orange G azo dye solutions by anodic oxidation with a boron-doped diamond anode in divided and undivided tank reactors. *Electrochimica Acta* **130**: 568-576.
13. **Fernández de la Ossa, M. Á., M. López-López, M. Torre, and C. García-Ruiz.** 2011. Analytical techniques in the study of highly-nitrated nitrocellulose. *TrAC Trends in Analytical Chemistry* **30(11)**: 1740-1755.
14. **Heilmann, H. M., U. Wiesmann, and M. K. Stenstrom.** 1996. Kinetics of the alkaline hydrolysis of high explosives RDX and HMX in aqueous solution and adsorbed to activated carbon. *Environmental Science & Technology* **30(5)**: 1485-1492.

15. **Jeong, J., C. Kim, and J. Yoon.** 2009. The effect of electrode material on the generation of oxidants and microbial inactivation in the electrochemical disinfection processes. *Water Research* **43(4)**: 895-901.
16. **Katsounaros, I., D. Ipsakis, C. Polatides, and G. Kyriacou.** 2006. Efficient electrochemical reduction of nitrate to nitrogen on tin cathode at very high cathodic potentials. *Electrochimica Acta* **52(3)**: 1329-1338.
17. **Kraft, A.** 2007. Doped diamond: A compact review on a new, versatile electrode material. *International Journal of Electrochemical Science* **2(5)**: 355-385.
18. **Kraft, A.** 2007. Doped diamond: A compact review on a new, versatile electrode material. *International Journal of Electrochemical Science* **2**: 355-385.
19. **Li, M., C. Feng, Z. Zhang, X. Lei, R. Chen, Y. Yang, and N. Sugiura.** 2009. Simultaneous reduction of nitrate and oxidation of by-products using electrochemical method. *Journal of Hazardous Materials* **171(1-3)**: 724-730.
20. **Li, X., H. Diao, F. Fan, J. Gu, F. Ding, and A. Tong.** 2004. Electrochemical wastewater disinfection: Identification of its principal germicidal actions. *Journal of Environmental Engineering* **130(10)**: 1217-1221.
21. **Li, X., F. Ding, P. Lo, and S. Sin.** 2002. Electrochemical disinfection of saline wastewater effluent. *Journal of Environmental Engineering* **128(8)**: 697-704.
22. **López-López, M., J. M. R. Alegre, C. García-Ruiz, and M. Torre.** 2011. Determination of the nitrogen content of nitrocellulose from smokeless gunpowders and collodions by alkaline hydrolysis and ion chromatography. *Analytica Chimica Acta* **685(2)**: 196-203.
23. **MacMillan, D. K., C. R. Majerus, R. D. Laubscher, and J. P. Shannon.** 2008. A reproducible method for determination of nitrocellulose in soil. *Talanta* **74(4)**: 1026-1031.
24. **Montanaro, D., E. Petrucci, and C. Merli.** 2008. Anodic, cathodic and combined treatments for the electrochemical oxidation of an effluent from the flame retardant industry. *Journal of Applied Electrochemistry* **38(7)**: 947-954.
25. **Monteil-Rivera, F., L. Paquet, R. Giroux, and J. Hawari.** 2008. Contribution of hydrolysis in the abiotic attenuation of RDX and HMX in coastal waters. *Journal Of Environmental Quality* **37(3)**: 858-864.
26. **Paquet, L., F. Monteil-Rivera, P. B. Hatzinger, M. Fuller, and J. Hawari.** 2011. Analysis of the key intermediates of RDX (hexahydro-1,3,5-trinitro-1,3,5-triazine) in groundwater: Occurrence, stability and preservation. *Journal Of Environmental Monitoring* **13(8)**: 2304-2311.
27. **Pelegriño, R. L., R. A. Di Iglia, C. G. Sanches, L. A. Avaca, and R. Bertazzoli.** 2002. Comparative study of commercial oxide electrodes performance in electrochemical degradation of organics in aqueous solutions. *Journal of the Brazilian Chemical Society* **13**: 60-65.
28. **Polatides, C., M. Dortsiou, and G. Kyriacou.** 2005. Electrochemical removal of nitrate ion from aqueous solution by pulsing potential electrolysis. *Electrochimica Acta* **50(25-26)**: 5237-5241.
29. **Poulin, I.** November 2010. Literature Review on Demilitarization of Munitions: Document Prepared for the RIGHTTRAC Technology Demonstration Project. Defence Research And Development Canada Valcartier (Quebec). Report# DRDC Valcartier TM 2010-213.
30. **Schaefer, C. E., C. Andaya, A. Urtiaga, E. R. McKenzie, and C. P. Higgins.** 2015. Electrochemical treatment of perfluorooctanoic acid (PFOA) and perfluorooctane sulfonic

- acid (PFOS) in groundwater impacted by aqueous film forming foams (AFFFs). *Journal of Hazardous Materials* **295**: 170-175.
31. **Scialdone, O.** 2009. Electrochemical oxidation of organic pollutants in water at metal oxide electrodes: A simple theoretical model including direct and indirect oxidation processes at the anodic surface. *Electrochimica Acta* **54(26)**: 6140-6147.
 32. **Su, T.-L., and Christodoulatos.** 1996. Destruction of nitrocellulose using alkaline hydrolysis. Tri-Service Environmental Technology Workshop. Hershey, PA, May 20-22.
 33. **Urriaga, A., C. Fernández-González, S. Gómez-Lavín, and I. Ortiz.** 2015. Kinetics of the electrochemical mineralization of perfluorooctanoic acid on ultrananocrystalline boron doped conductive diamond electrodes. *Chemosphere* **129**: 20-26.
 34. **Wang, C.-T., W.-L. Chou, Y.-M. Kuo, and F.-L. Chang.** 2009. Paired removal of color and COD from textile dyeing wastewater by simultaneous anodic and indirect cathodic oxidation. *Journal of Hazardous Materials* **169(1)**: 16-22.
 35. **Wilkinson, J., and D. Watt.** January 2006. Review Of Demilitarisation And Disposal Techniques For Munitions And Related Materials. Munitions Safety Information Analysis Center. Report# L-118.
 36. **Wolf, F. E.** 1997. Alkaline hydrolysis conversion of nitrocellulose fines. Olin Corporation, Badger Army Ammunition Plant. Report# 19980218 030.
 37. **Xu, F., M. Kameche, and C. Innocent.** 2012. Transport of ions and solvent through a Nafion membrane modified with polypyrrole. *Journal of Membrane and Separation Technology* **1(2)**: 108-116.
 38. **Yavuz, Y., and A. S. Koparal.** 2006. Electrochemical oxidation of phenol in a parallel plate reactor using ruthenium mixed metal oxide electrode. *Journal of Hazardous Materials* **136(2)**: 296-302.
 39. **Yu, J., and M. J. Kupferle.** 2008. Two-stage sequential electrochemical treatment of nitrate brine wastes. *Water, Air, & Soil Pollution: Focus* **8(3)**: 379-385.

5.0 APPENDICES

A. Other Supporting Data – N/A

B. List of Scientific/Technical Publications

Articles in peer-reviewed journals (planned)

Fuller, M. E., C. Andaya, P. Koster van Groos, and C. E. Schaefer. Electrochemical degradation of solid nitrocellulose using a mixed metal oxide (MMO) anode and stainless steel cathode.

Fuller, M. E., C. Andaya, and C. E. Schaefer. Evaluation of boron doped diamond and mixed metal oxide (MMO) electrodes for degradation of dissolved explosives.

Conference or symposium abstracts

Fuller, M. E., C. Andaya, P. Koster van Groos, and C. E. Schaefer. 2017. *Electrochemical Demilitarization Of Energetics*. SERDP ESTCP Symposium. Washington, D.C., USA, November 28-30.

The efficient and safe destruction of waste munition constituents is an ongoing issue across the DoD. The key objective of this project is to demonstrate electrochemical treatment of several representative explosive and propellant compounds at the bench-scale. Specific attention is being given to determining the overall rates of treatment, delineating the major transformation products of the process, and assessing the ability to effectively treat slurried and solid phase explosives and propellants.

The technical approach for this project includes screening level testing to select the appropriate electrode / electrolyte combination and operational parameters to effectively destroy the target energetic materials. Results with RDX (as a model explosive compound) indicated reactions at the electrode surface may dominate the degradation process, although alkaline hydrolysis during divided cell operation may also be involved. In contrast, degradation of nitrocellulose (as a model propellant) during divided cell operation was predominantly via alkaline hydrolysis through in situ hydroxide generation.

The proposed technology offers DoD a means to address demilitarization wastestreams in a manner that does not require the use of dangerous reactive chemicals or environmentally unfriendly processes. The oxidants required to degrade the energetics are generated in the system, without the need to store and handle large amounts of caustic or reactive substances on site. Additionally, at the pilot and full-scale, the energy demands of the technology may be offset by capture and use of hydrogen off-gas in a fuel cell, and/or powering the electrochemical cell using solar irradiation. The latter would also allow the technology to be deployed in more remote areas where some demilitarization activities may be located due to safety concerns.